Recent Development of CDK2 Inhibitors as Anticancer Drugs: An Update (2015–2023)

Yumei Jin[1#] Hao Lu[1#] Hu Ge[2] Xuben Hou[1*] Hao Fang[1*]

[1] Department of Medicinal Chemistry, Key Laboratory of Chemical Biology, School of Pharmaceutical Science, Cheeloo College of Medicine, Shandong University, Ji'nan, Shandong, People's Republic of China
[2] Wecomput Technology Co., Ltd., Shanghai, People's Republic of China

Pharmaceut Fronts 2024;6:e195–e220.

Address for correspondence Xuben Hou, PhD, School of Pharmaceutical Science, Cheeloo College of Medicine, Shandong University, 44 Wenhuaxi Road, Ji'nan 250012, People's Republic of China (e-mail: hxb@sdu.edu.cn).

Hao Fang, PhD, School of Pharmaceutical Science, Cheeloo College of Medicine, Shandong University, 44 Wenhuaxi Road, Ji'nan 250012, People's Republic of China (e-mail: haofangcn@sdu.edu.cn).

Abstract

Cyclin-dependent kinase 2 (CDK2) is a critical regulator of cell division and has emerged as a promising target for anticancer treatment. In this article, we summarize the structural features of CDK2 inhibitors and corresponding binding modes, in particular the noncompetitive binding modes that offer unique advantages for the development of highly selective inhibitors. In addition, we present an overview of the latest advancements in the development of CDK2 inhibitors and discuss the trend in the field. This review provides valuable insights into the structure–activity relationships of the reported CDK2 inhibitors, inspiring the development of potent and selective CDK2 inhibitors in the future.

Keywords
- cyclin-dependent kinase 2
- non-ATP competitive inhibitor
- anticancer drugs

Introduction

Cyclin-dependent kinases (CDKs) are a group of serine/threonine kinases that interact with regulatory subunits called cyclins to exert their activity.[1,2] These CDKs are crucial in regulating cell-cycle progression and transcription (►**Fig. 1**).[3,4] Twenty CDKs (CDK1–20) and 29 cyclins have been identified in human cells.[5] Among them, CDK1, CDK2, CDK4, and CDK6 play key roles in cell-cycle regulation, whereas CDK7–9, 11–13, 19, and 20 play key roles primarily in transcriptional regulation.[2,4,6,7] It is worth noting that many CDKs have multiple catalytic substrates and are involved in various cellular processes. For example, CDK7 is a kinase that activates CDKs during the cell cycle and a regulator of RNA polymerase II during transcription. CDK5 is widely recognized as a crucial factor in regulating neuronal function and cell migration.[8] A hallmark feature of cancer is the dysregulation of the cell cycle leading to uncontrolled and excessive cell growth.[9] CDKs regulate the different phases of the cell cycle and have been potential targets for cancer therapy.[10]

The development of CDK inhibitors has been extensively investigated. However, the first-generation inhibitors lack specificity for specific CDK members and mainly act as pan-CDK inhibitors. Despite the initial interest from preclinical studies, pan-CDK inhibitors have limited therapeutic efficacy, leading to the termination of a large number of clinical trials involving them. Recognizing the need for selective CDK inhibitors, researchers have focused on the development of second- and third-generation inhibitors, through comprehensive research on the structure of the inhibitors and their biological functions. Palbociclib (Ibrance), the first CDK4/6-selective inhibitor, was approved by the Food and Drug Administration (FDA) in 2015, followed by ribociclib (Kisqali), abemaciclib (Verzenio) and trilaciclib (Cosela), approved by FDA in 2017, and dalpiciclib approved by the National Medical Products Administration in 2021 (►**Fig. 2**).[11–15] These new-generation CDK4/6 inhibitors exhibit improved selectivity and reduced cytotoxicity compared with the first-generation pan-CDK inhibitor, flavopiridol (►**Fig. 2**).[14,16]

[#] *These authors contribute equally to this work.*

received
December 5, 2023
accepted
August 1, 2024
article published online
September 3, 2024

DOI https://doi.org/10.1055/s-0044-1789577.
ISSN 2628-5088.

Georg Thieme Verlag KG, Rüdigerstraße 14, 70469 Stuttgart, Germany

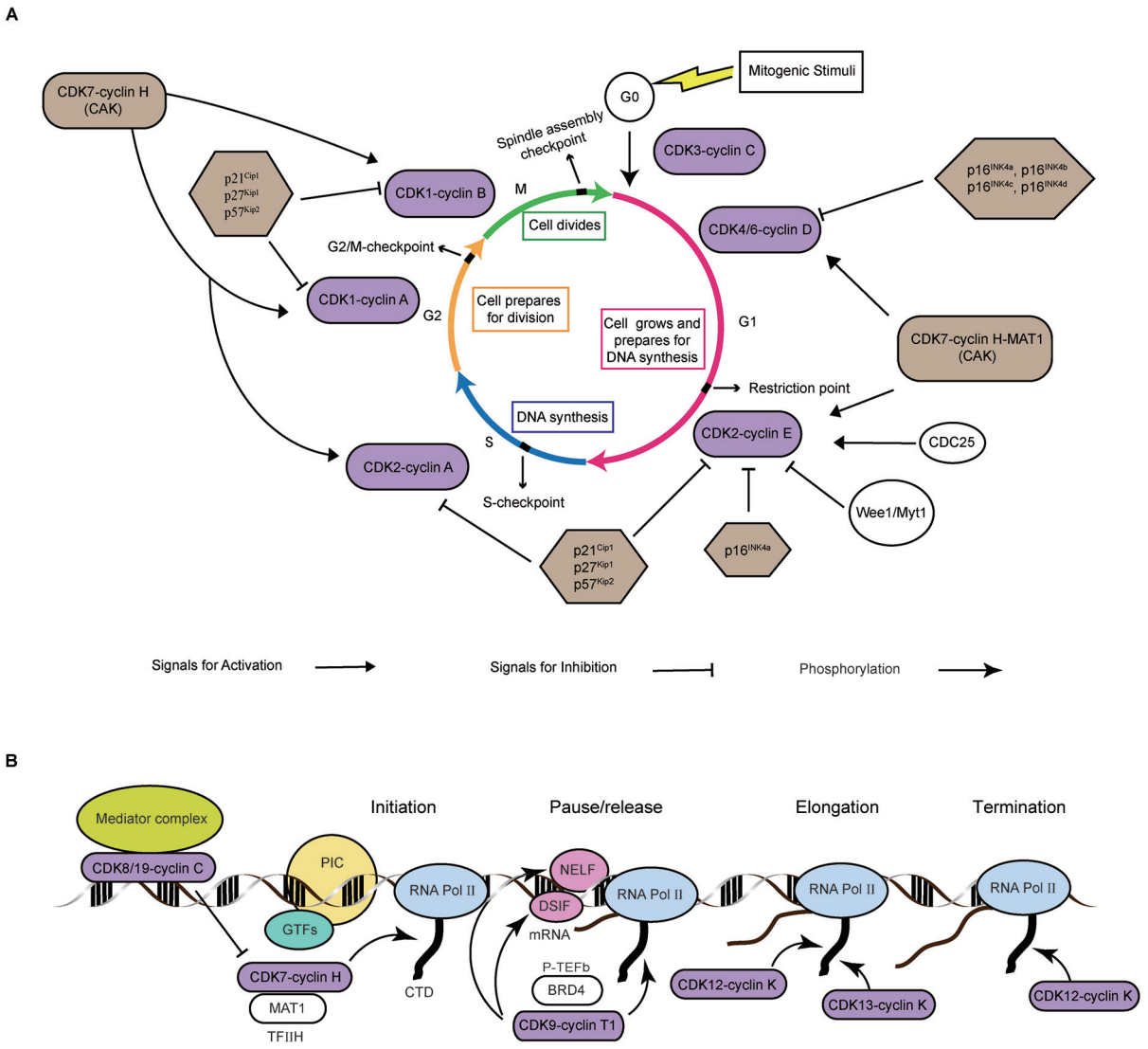

Fig. 1 Functions of CDKs in cell-cycle progression and transcription regulation. (**A**) CDKs in cell-cycle progression: mitogenic stimuli in quiescent (G0) cells activate the CDK3–cyclin C complex to stimulate the phosphorylation of Rb, promoting the G0/G1 transition. Sequential phosphorylation of Rb by CDK4/6–cyclin D and CDK2–cyclin E leads to E2F transcription factor activation, facilitating the G1/S transition through the restriction point. As cells approach the end of the S phase, CDK2–cyclin A directly phosphorylates E2Fs, inactivating its function and promoting S phase completion while preventing cell apoptosis due to sustained E2F activity. CDK1–cyclin A and CDK1–cyclin B complexes play a crucial role in the passage of the G2/M checkpoint and cell division progression. (**B**) CDKs in transcription regulation: the binding of mediator complex and CDK8 (or the highly related CDK19) promotes transcription activation and regulates gene expression from super-enhancers. Transcription-associated CDKs phosphorylate the CTD of RNA polymerase II (RNA Pol II). CDK7, CDK12, and CDK13 directly phosphorylate the CTD of RNA Pol II, regulating distinct phases of transcript generation, including initiation, pause/release, elongation, and termination. CDKs, cyclin-dependent kinases; CTD, C-terminal domain.

Cyclin-dependent kinase 2 (CDK2), a member of the CDK family, regulates cell-cycle progression, and its dysregulation leads to uncontrolled cell proliferation and subsequent cancer progression and metastasis. It primarily drives the proliferation of specific tumor types with defined genetic characteristics, including ovarian cancers, MYC-overexpressed cancers, and melanoma.[17,18] Elevated expression of CDK2 and its associated cyclins have been observed in many types of cancers, highlighting CDK2 as a promising target for drug discovery.[19]

There are significant challenges in developing CDK2-selective inhibitors due to the sequence and structural similarity of CDK2 to other CDKs. For instance, CDK2 shares 65% sequence similarity with CDK1, and they have minimal differences in their adenosine triphosphate (ATP)-binding pockets.[20,21] This article reviewed the structure and function of CDK2 inhibitors, with a special focus on noncompetitive CDK2 inhibitors, aiming to provide new insights and guidance for the future development of CDK2-selective inhibitors that meet the necessary criteria for clinical application.

The Structure of CDK2 and the Regulation of Its Enzymatic Activity

CDK2 is a typical bilobed structure with a molecular weight of 34 kDa and is composed of 298 amino acids. The protein consists of a smaller N-terminal lobe (residues 1–85) and a

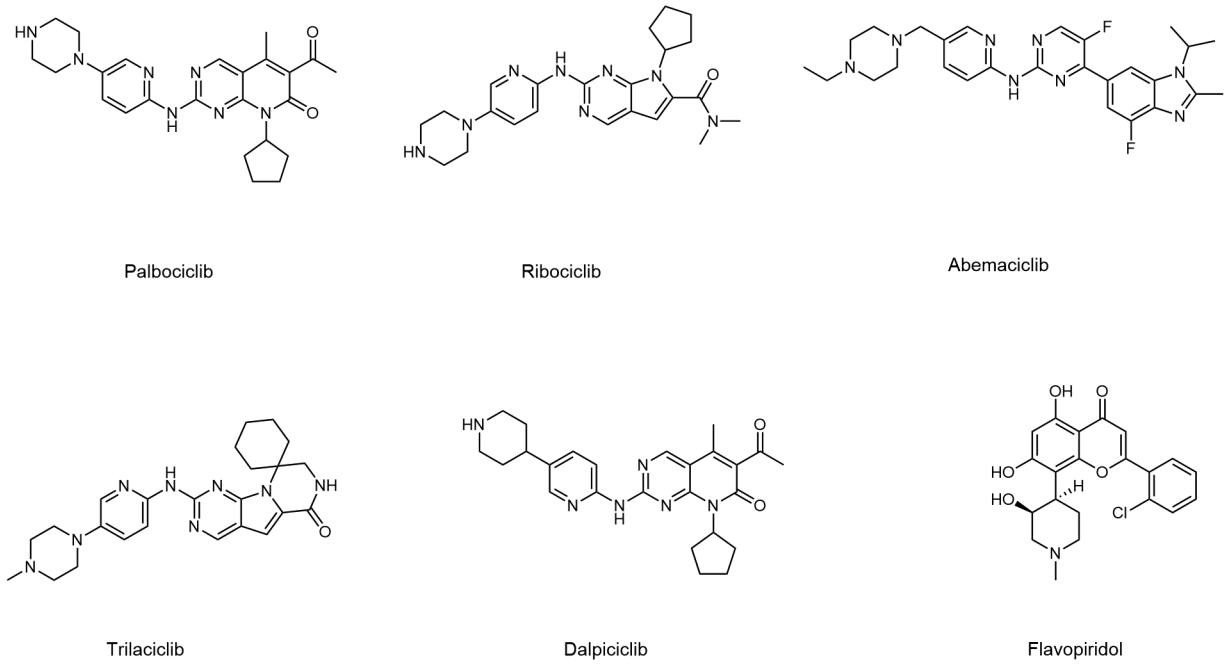

Fig. 2 Structures of marketed CDK4/6-selective inhibitors and the first-generation CDK inhibitor, flavopiridol.

larger C-terminal lobe (residues 86–298). The N-terminal lobe contains five antiparallel β-sheets and a single αC-helix, while the C-terminal lobe is rich in α-helices (►**Fig. 3**).[22] The two lobes are connected by a flexible hinge or linker region, spanning residues 81–83. The three parts form a narrow, deep lipophilic cleft that serves as the ATP-binding site.[17,22] Most of the currently developed CDK2 inhibitors bind to this site and are therefore classified as type I inhibitors in the family of protein kinase inhibitor.[1,17]

CDK2 exists as an inactive monomeric form in mammalian cells and requires a series of complex activation processes to achieve a stable and fully activated conformation. This involves binding to cyclin A/E and the subsequent phosphorylation of Thr160 (►**Fig. 4**). Wee1 and Myt1 kinases induced the phosphorylation of Thr14 and Tyr15 within the glycine-rich loop (residues 8–18), leading to inactivation of CDK2–cyclin A/E, which can be reversed by the cell division cycle 25 (CDC25) phosphatases (CDC25A, CDC25B, and CDC25C). The activity of CDK2 can be lost by binding to endogenous inhibitors (Cip and Kip protein).[20,23]

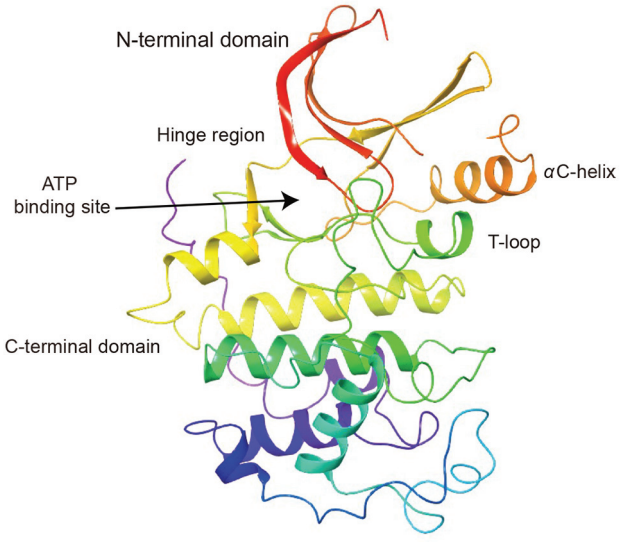

Fig. 3 Crystal structure of monomeric CDK2 (PDB ID: 1HCL).

The Biological Activity of CDK2

CDK2 is a fundamental component of the cell cycle in dividing cells, exhibiting crucial activity starting from the late G1 phase and persisting throughout S-phase.[20] It regulates multiple processes, including centrosome duplication, DNA synthesis, G1/S transition, and the regulation of G2 progression during the cell division cycle (►**Fig. 5**).[24] When cells in the quiescence (G0) enter the cell cycle, the transcription of cyclin D is promoted by the extracellular signals, leading to the formation of CDK4/6–cyclin D (D1, D2, and D3) complexes.[24] The active CDK4/6–cyclin D complexes induce partial phosphorylation of the retinoblastoma (Rb) protein in the G1 phase, leading to the activation of E2F transcription factors (E2Fs). The phosphorylation of the Rb protein is significant in the late G1 phase through interaction between cyclin E and CDK2, promoting the release of E2Fs and their full activation. Consequently, E2Fs translocate into the nucleus and stimulate the transcription of cyclin E and cyclin A. CDK2 is stable and continuously expressed throughout the cell cycle.[25] The activated CDK2–cyclin E complex phosphorylates substrate factors such as Rb, CDC6, NPAT, and P107, which enables cells to initiate DNA and histone synthesis, facilitates the passage of the G1/S checkpoint, and ensures smooth and irreversible entry into the S phase.[25,26] At the same time, CDK2–cyclin E contributes to the phosphorylation of specific centrosome proteins, including

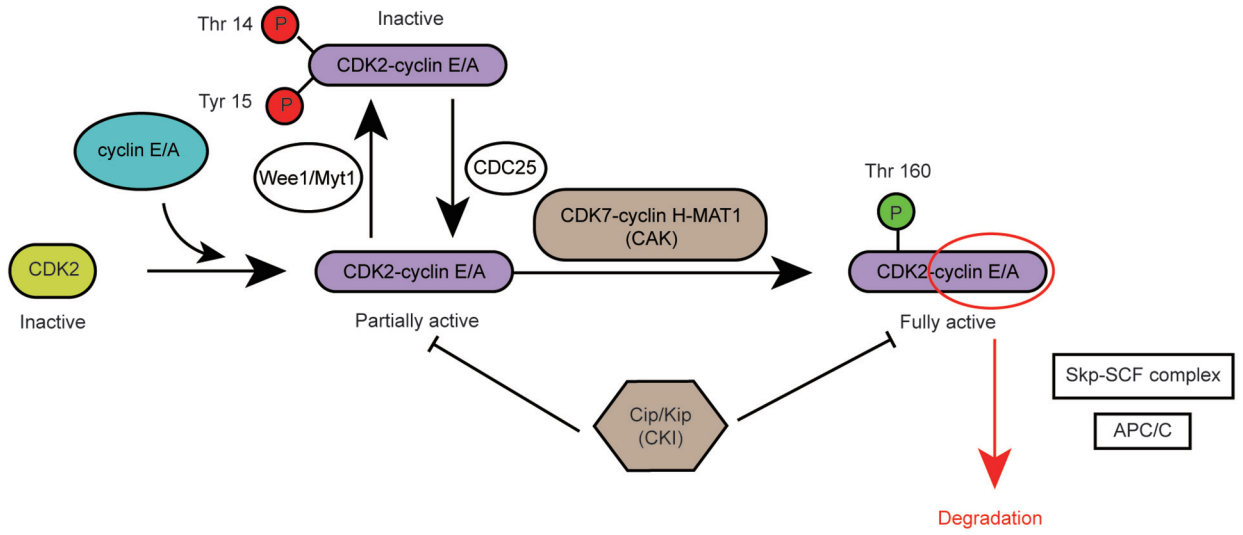

Fig. 4 The activity of CDK2 is regulated by multiple mechanisms. Binding of CDK2 to cyclin E and A forms partially activated CDK2–cyclin E and CDK2–cyclin A complexes, which require further phosphorylation on Thr160 by the CDK7–cyclin H-MAT1 (CAK) complex for full activation. Additionally, inhibitory phosphorylation on Thr14 and Tyr15 by Wee1 and Myt1 kinases results in the loss of CDK2–cyclin complex activity. However, the dephosphorylation of these sites by the CDC 25 (cell division cycle 25) family could restore the activity of CDK2. Finally, the binding of CDK2 to the endogenous CDK inhibitory protein family (Cip and Kip protein) could lead to its inactivation. Cyclin E and A are ubiquitinated and degraded by the Skp2–SCF complex and APC/C. APC/C, anaphase-promoting complex/cyclosome; Skp2–SCF, S-phase kinase-associated protein 2-skp-cullin-F-box protein.

nucleophosmin (NPM/B23) and centriolar coiled-coil protein of 110 kDa (CP110), leading to the initial release of centrioles and subsequent centriole duplication.[27,28]

CDK2 controls the G1/S transition of the cell cycle. It is activated through binding to cyclin E in the late G1 phase and binding to cyclin A in the S phase.[29] In the S phase, S-phase kinase-associated protein 2 (Skp2) and SCF complex (Skp-cullin-F-box protein) form the Skp2–SCF complex, which mediates the ubiquitinated degradation of cyclin E (►**Fig. 4**).[20,25] At the same time, cyclin A replaces cyclin E and binds to CDK2. In the early S phase, activation of CDK2–cyclin A promotes the phosphorylation of multiple endogenous substrates, facilitates DNA replication, and subsequently inactivates E2Fs.[30] As the cells approach the end of the S phase, the CDK2–cyclin A complex phosphorylates E2Fs directly, thereby, inhibiting their functions. The phosphorylation event is essential to complete the S phase and prevent apoptosis that may be induced by sustained E2F activity in the absence of the CDK2–cyclin A complex.[20,24,31] The S phase is terminated by the CDK2–cyclin A complex, which drives the transition of the cell cycle from the S phase to the G2 phase by phosphorylating CDC6 and E2Fs. Subsequently, CDK1 is activated by cyclin A, initiating the cells into the M phase.[5]

CDK2, like other kinases, phosphorylates substrates using ATP as a phosphate donor.[30] CDK2 phosphorylates various transcription factors involved in different stages of cell-cycle progression.[20] In addition to regulating the cell cycle, CDK2 is involved in a variety of biological processes, including cell differentiation,[32] chromosomal instability,[33–35] adaptive immune response,[36,37] cell senescence,[38–40] cell metabolism,[41] cell apoptosis,[42–45] virus replication,[46,47] spermatogenesis,[48–51] hearing loss,[52] etc. (►**Fig. 5**).

CDK2 Inhibitors

The activation of CDK2 is accompanied by a series of changes of its structure including the rotation of C-helix and the migration of T-loop. These changes generate numerous new binding sites. Depending on the binding site, CDK2 inhibitors can be classified into four categories (type I, II, III, and IV inhibitors). Type I inhibitors bind to the ATP-binding site and target an active kinase state characterized by an αC helix-in and DFG (conserved tripeptide Asp-Phe-Gly) motif-in conformation. Type II inhibitors target the ATP-binding site but focus on an inactive kinase state characterized by an αC helix-in and DFG motif-out conformation. Type III inhibitors bind near the ATP-binding site within a pocket formed by an αC helix-out conformation, with an active "in" conformation of the DFG motif. Type IV inhibitors, on the other hand, bind to allosteric sites located at a distance from the ATP-binding site.[53,54]

Type I Inhibitors (ATP-Competitive Inhibitors)

The lack of selectivity of CDK2 inhibitors is due to the ATP-binding pocket is highly conserved across 518 members of the human genome, and the fact that other cellular enzymes also can bind ATP.[55] ATP has three binding regions: the adenine-binding region, the ribose-binding region, and the phosphate-binding region (►**Fig. 6**). The hinge region contains hydrogen bond donor and acceptor sites including the carbonyl oxygen of Glu81, and the carbonyl oxygen and the nitrogen atom of Leu83 which can establish hydrogen bonds with the adenine ring of ATP. Therefore, many inhibitors are designed and synthesized with adenine rings, such as NU2508 and CVT313, based on the structural features of ATP. Unfortunately, these inhibitors are not selective but pan-

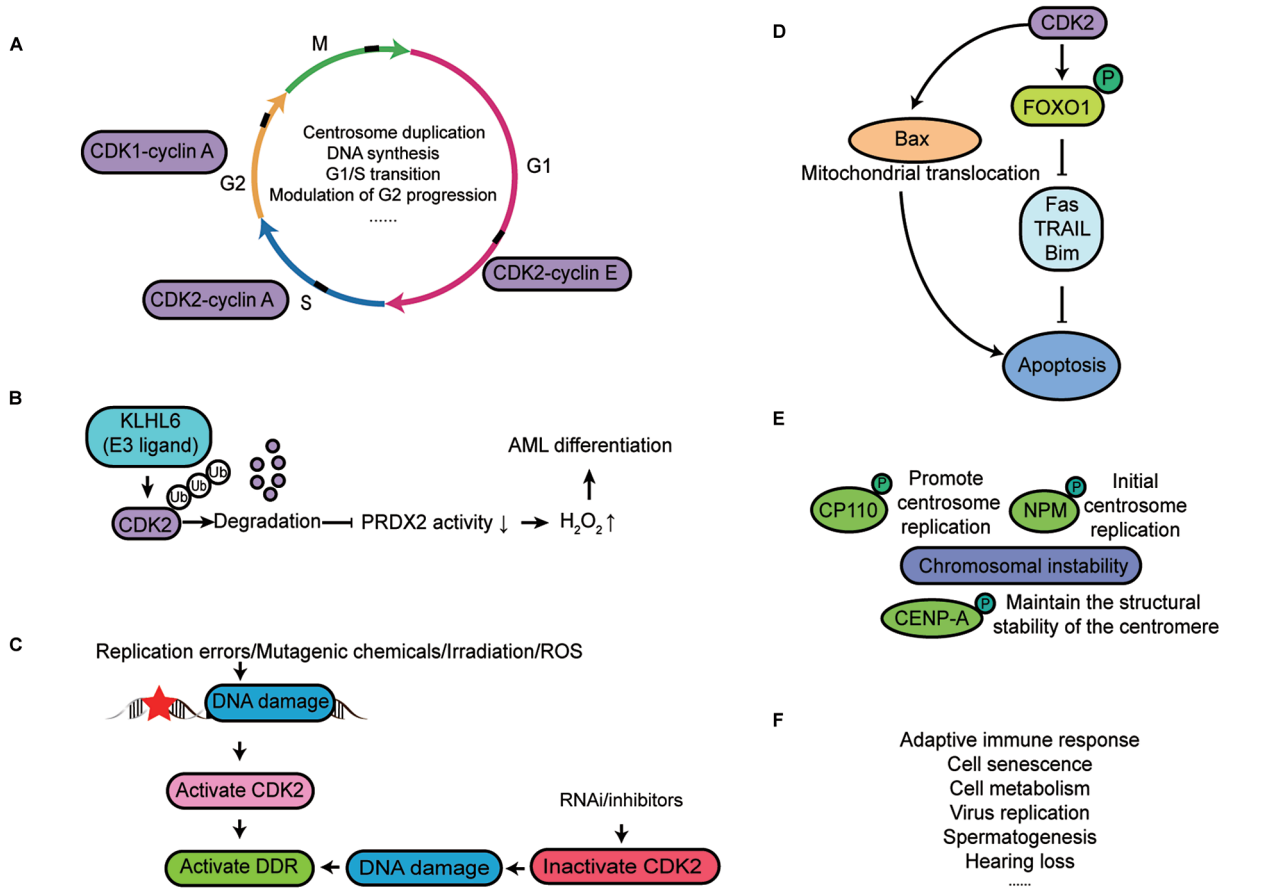

Fig. 5 CDK2 biological functions. (**A**) The roles of CDK2 in regulating multiple processes during the cell division cycle, including centrosome duplication, DNA synthesis, G1/S transition, and modulation of G2 progression. (**B**) The ubiquitin E3 ligase KLHL6 can ubiquitinate CDK2 and mediate its specific degradation. Depletion or knockdown of CDK2 protein can downregulate the activity of peroxiredoxin PRDX2, promoting the accumulation of H_2O_2 and contributing to the differentiation of acute myeloid leukemia cells. (**C**) The dual role of CDK2 in DNA damage and response. (**D**) CDK2 regulates cell apoptosis through various mechanisms, including activation of apoptosis by promoting mitochondrial translocation and loss of mitochondrial transmembrane potential of Bax, as well as inhibition of DNA damage-induced apoptosis by phosphorylating the transcription factor FOXO1 to suppress the expression of downstream pro-apoptotic genes. (**E**) Abnormal centrosome or centromere function can lead to chromosomal segregation abnormalities, resulting in chromosomal instability. (**F**) The unique roles of CDK2 in biological processes, including adaptive immune response, cell senescence, cell metabolism, virus replication, spermatogenesis, and hearing loss. FOXO1, forkhead box protein O1.

inhibitors. In addition, most CDK2 inhibitors including NU6102 are dual CDK1/2 inhibitors due to the high structural similarity between CDK1 and CDK2. However, CDK1 inhibition is closely associated with toxicity. Therefore, it is crucial to improve the selectivity of CDK2.[7]

Purine-Based CDK2 Inhibitors

Anscombe et al designed and synthesized NU6300 (compound **1**, ►**Table 1**) as a selective CDK2 inhibitor in 2015,[56] which provides an alternative route to ATP-competitive inhibitors that target protein kinases. NU6300 was initially identified as the first covalent CDK2 inhibitor. Subsequent modifications were made to NU6102, substituting the sulfanilamide group with vinyl sulfones, leading to a selective CDK2 inhibitor, suggesting the potential roles of vinyl sulfones in designing selective compounds.[56] Besides, the high selectivity of the inhibitors is attributed to their covalent attachment to the Lys89 residue of CDK2. The vinyl moiety reacts with the ε-amino group on Lys89 located outside the CDK2 ATP-binding cleft, which is not highly conserved among protein kinases.[56]

NU6102 was further optimized to produce CDK2-IN-4 (compound **2**, ►**Table 1**), a novel compound belonging to the class of 6-substituted 2-(4'-sulfamoylanilino)purines. Compound **2** demonstrates high selectivity toward CDK2 (IC_{50} = 44 nmol/L), exhibiting approximately 2,000-fold selectivity over CDK1 (IC_{50} = 86 μmol/L). Co-crystal structures reveal that the inhibitor stabilizes the conformation of the glycine-rich loop, shaping the ATP ribose binding pocket. The characteristic of the specific binding site may be used to develop inhibitors that differentiate between CDK1 and CDK2.[57]

In 2020, Köprülüoğlu et al developed a class of novel compounds that replaced the 9-position purine scaffold with a norbornyl moiety. Among these compounds, **3** (►**Fig. 7**) was the most potent inhibitor, with an IC_{50} value of 190 nmol/L, specifically targeting the CDK2/cyclin E complex. The 9-hydroxymethyl norbornyl moiety establishes π–π interactions with the Phe80 gatekeeper, and its terminal hydroxyl group forms two hydrogen bonds with Lys33 and Glu51.[58] Norbornyl-based carbocyclic nucleoside derivatives

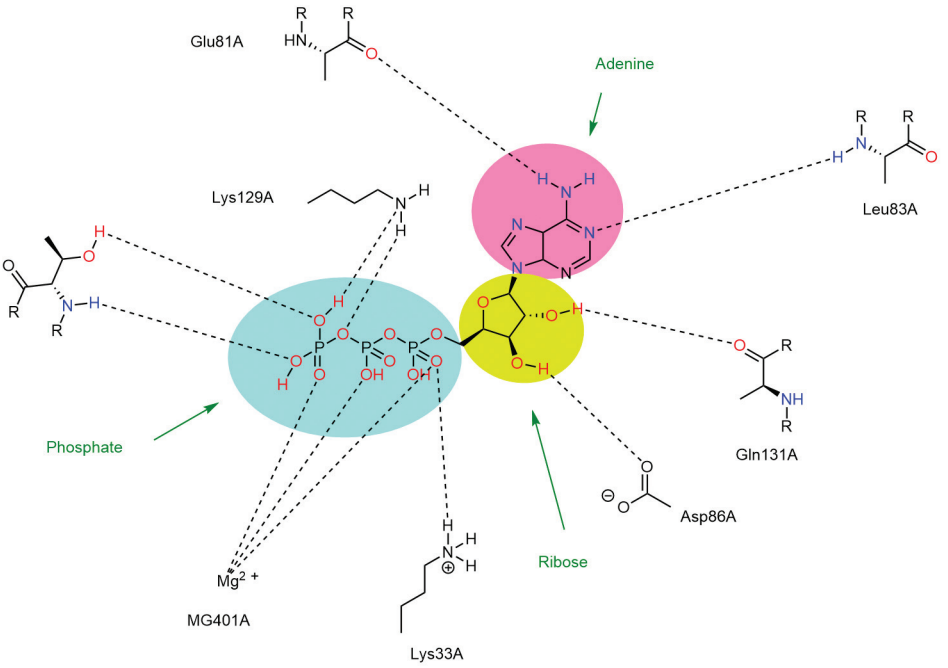

Fig. 6 ATP binds to residues of CDK2.

offer a vast scope for the development of powerful CDK2 inhibitors.

Inspired by two previously identified CDK inhibitors, dinaciclib and Cmpd-27, Park et al developed a novel 6-aminopurine scaffold incorporating an N9-*cis*-cyclobutyl moiety using a structural-based molecular design method. Compound **4** significantly inhibited CDK2 and CDK5 with IC_{50} values of 2.1 and 4.8 nmol/L, respectively (►**Fig. 7**), and exhibited moderate antiproliferative effect against HCT116 and MCF7 cancer cell lines.[59]

Table 1 The structures of purine-based CDK2 inhibitors

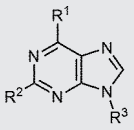

Compd.	Structure	IC_{50} (μmol/L) for CDKs	Ref.
NU6300	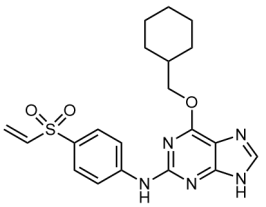	CDK2: 0.16	56
CDK2-IN-4	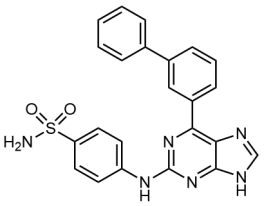	CDK1/cyclin B: 86 CDK2/cyclin A: 0.044 CDK4/cyclin D: 26 CDK7/cyclin H: 28 CDK9/cyclin T: 25	57
CVT313	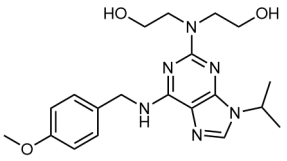	CDK2/cyclin A: 0.5 CDK1/cyclin B: 4.2 CDK4/cyclin D1: 215	61

Table 1 (*Continued*)

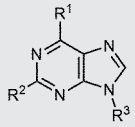			
Compd.	**Structure**	**IC_{50} (μmol/L) for CDKs**	**Ref.**
Roscovitine	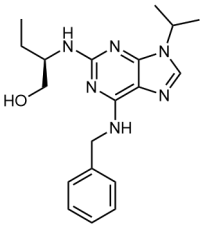	CDK2/cyclin B: 0.65 CDK2/cyclin A: 0.7 CDK2/cyclin E: 0.7 CDK4/cyclin D1: >100 CDK5/p35: 0.16 CDK6/cyclin D3: >100	62
CYC065	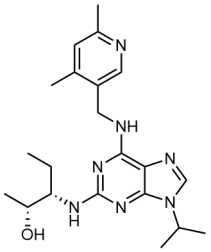	CDK2: 0.005 CDK9: 0.026	63
Purvalanol A	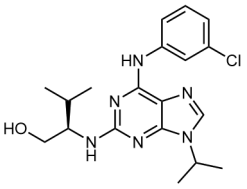	CDK2/cyclin B: 0.004 CDK2/cyclin A: 0.070 CDK2/cyclin E: 0.035 CDK4/cyclin D: 0.850 CDK5/p35: 0.075	64
Purvalanol B	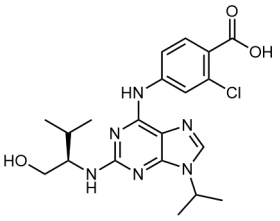	CDK2/cyclin B: 0.006 CDK2/cyclin A: 0.006 CDK2/cyclin E: 0.009 CDK4/cyclin D: >10 CDK5/p35: 0.006	64
(R)-CR8	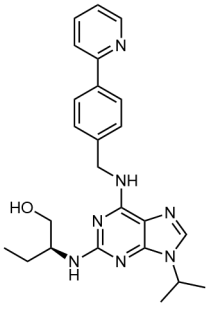	CDK1/cyclin B: 0.09 CDK2/cyclin A: 0.072 CDK2/cyclin E: 0.041 CDK5/p25: 0.11 CDK7/cyclin H: 1.10 CDK9/cyclin T: 0.18	65
NU2058	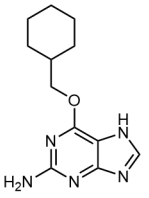	CDK2: 17 CDK1: 26	66

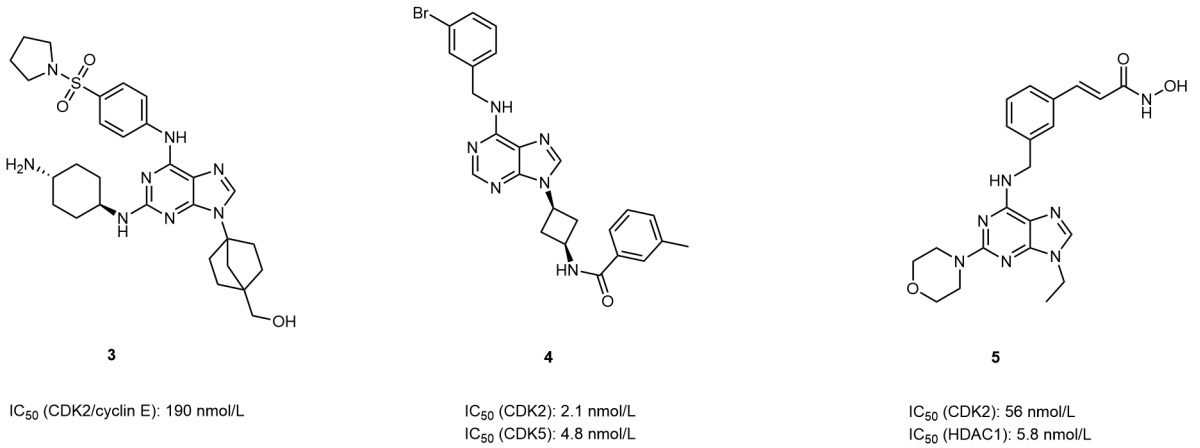

Fig. 7 The structures of compound **3**, **4**, and **5**.

Compound **5**, a 9*H*-purine derivative developed based on a pharmacophore design strategy, is a dual inhibitor of HDAC1 and CDK2, with IC_{50} values of 5.8 and 56 nmol/L, respectively (►**Fig. 7**). The compound significantly inhibits the proliferation of several human tumor cell lines, including human lung cancer cell line A549 cells ($IC_{50} = 1.49 \pm 0.07$ µmol/L), human liver cancer cell line HepG2 cells ($IC_{50} = 0.77 \pm 0.07$ µmol/L), and human breast cancer cell line CAL-148 cells ($IC_{50} = 1.14 \pm 0.21$ µmol/L). The hydroxamic acid group, which can form hydrogen bonds with HDAC1, also exhibits strong hydrogen bonding interactions with Glu8 and Lys20 residues in molecular docking studies involving CDK2. These interactions contribute to the potent activity of **5** against CDK2.[60]

The structures of other representative purine-based CDK2 inhibitors and their activity against CDKs are summarized in ►**Table 1**.[56,57,61–66]

Pyrimidine-Based CDK2 Inhibitors

Dinaciclib (compound **6**, ►**Fig. 8**) is a compound with a pyrazolo[1,5-*a*]pyrimidine (PP) scaffold and exhibits very high potency against CDK1, CDK2, CDK5, and CDK9 (nanomolar activity with $IC_{50} = 1–4$ nmol/L). It is currently in phase 3 clinical trials,[67] unfortunately, it is a pan-CDK inhibitor, and lacks selectivity. Pharmacokinetic studies have shown that **6** has a short plasma half-life ($t_{1/2}$) in mice. When **6** (5 mg/kg) was administered to mice intravenously, it had a $t_{1/2}$ of approximately 0.25 hours. In addition, **6** demonstrates dose-dependent antitumor activity *in vivo*, and at dose levels below the maximum tolerated dose (MTD), it inhibited tumor growth almost completely. Analysis of mouse plasma samples collected at different times after intraperitoneal injection of **6** (5 mg/kg) revealed an area under the curve (AUC) of 0.8 µmol/L·h and a maximum concentration (C_{max}) of 0.8 µmol/L. Encouragingly, the compound was effective against a variety of *in vivo* xenografts including thyroid, pancreatic cancer, T cell acute lymphoblastic leukemia, neuroblastoma, melanoma, etc.[68–73]

Recent research has focused on exploring a class of novel selective CDK2 inhibitors with a PP scaffold. The most potent compound **7** demonstrated an IC_{50} value of 15 nmol/L.[74] The PP scaffold features a biphenyl substituent, which extends into an unexplored pocket and illustrates the impact of the active site-waters on the affinity (►**Fig. 8**).[74]

The compounds with a pyrazolo[3,4-*d*]pyrimidine scaffold exhibit moderate inhibitory activity against CDK2, with IC_{50} values in the micromolar range (►**Fig. 9**). Among those compounds, **8** containing a benzenesulfonamide moiety showed an IC_{50} value of 0.19 µmol/L, which is in a submicromolar range. Besides, **8** significantly inhibited the proliferation of the HepG2 cell line ($IC_{50} = 0.40$ µmol/L) and can arrest the cell cycle at the S and G2/M phases; moreover, it upregulates the expression of endogenous inhibitors p21 and p27 of CDK2.[75–77]

The compounds with a pyrazolo[4,3-*d*]pyrimidine scaffold that could form three hydrogen bonds with the hinge

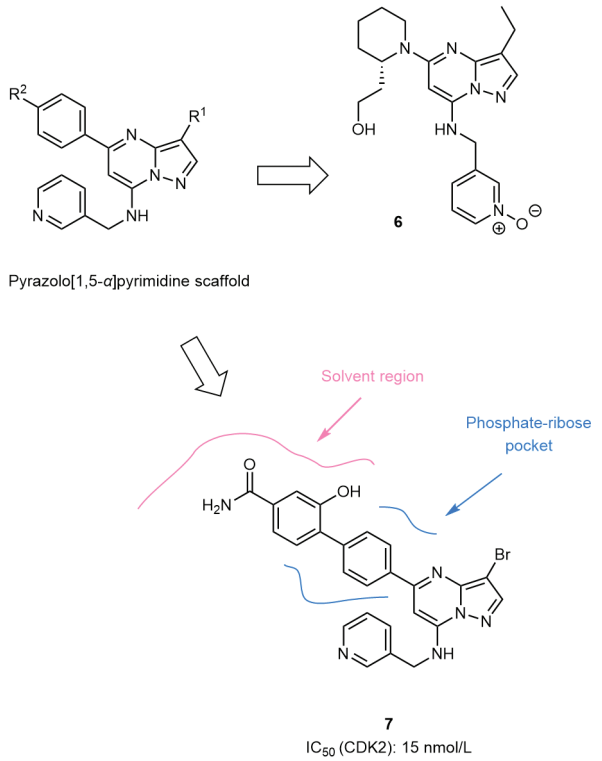

Fig. 8 Modifications of the pyrazolo[1,5-*a*]pyrimidine scaffold.

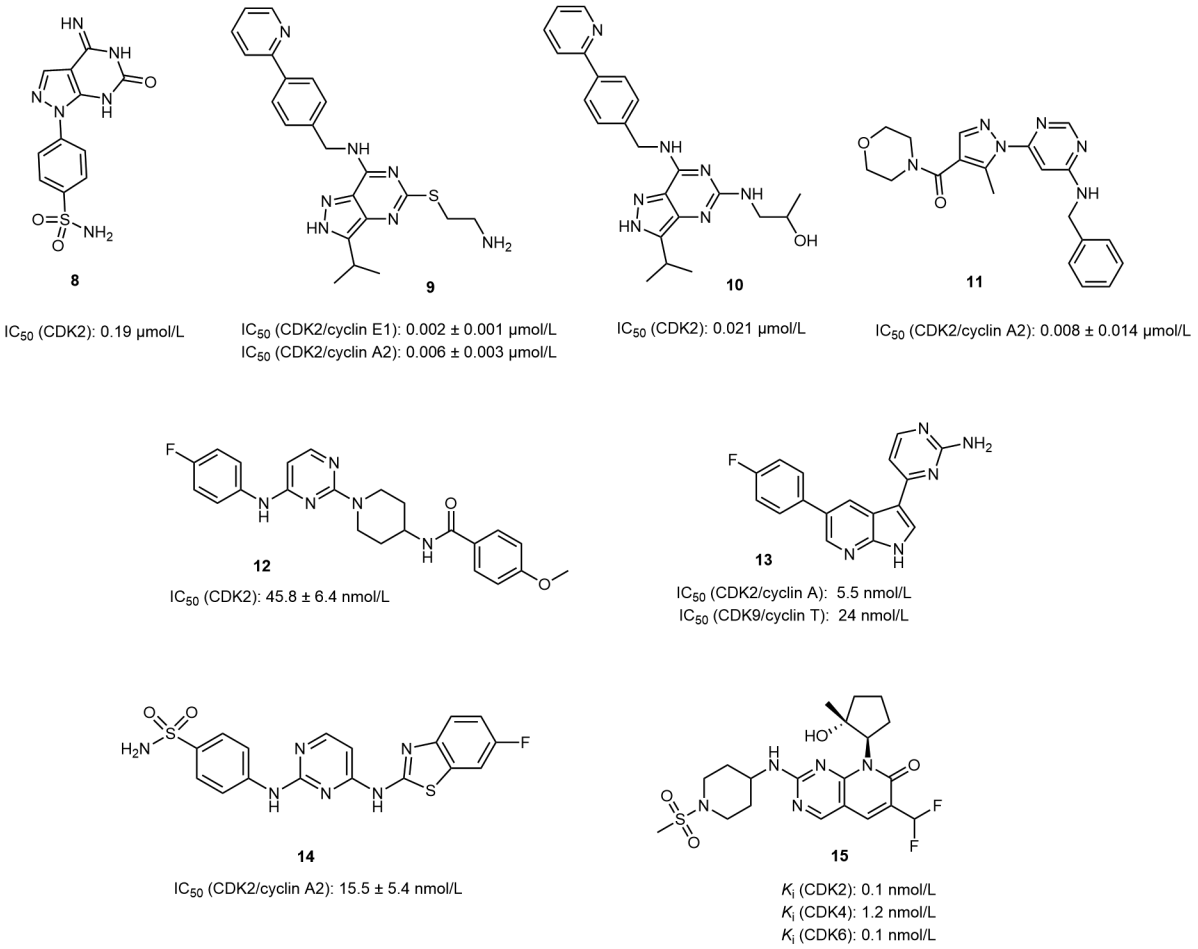

Fig. 9 The structures of compounds **8–15**.

region may lead to a higher potent. Compound **9** (►**Fig. 9**) is an effective analog with a pyrazolo[4,3-*d*]pyrimidine scaffold that targets CDK2/cyclin E1 and CDK2/cyclin A2 with IC_{50} values of 0.002 ± 0.001 and 0.006 ± 0.003 μmol/L, respectively. Compound **9** has broad antiproliferative activity against human cancer cell lines, including lymphoma cell lines, breast cancer cell lines, cervix cancer cell lines, etc., and is more selective than dinaciclib. Compound **9** displays relatively fast pharmacokinetics and limited oral availability, with approximately 40% of the drug being metabolized 1 hour after intravenous administration. Compound **9** significantly reduces tumor growth in subcutaneous xenografts of three types of lymphoma cell lines and a patient-derived lymphoma in monotherapy, while downregulating the expression of MCL-1 and XIAP proteins. Additionally, **9** significantly inhibited tumor growth in the MAVER-1 xenograft animal model combined with venetoclax (ABT-199), an inhibitor of BCL-2 family proteins.[78]

Compound **10** (►**Fig. 9**) showed strong inhibitory activity against CDK2, with an IC_{50} value of 0.021 μmol/L. The enhanced activity may be attributed to a biarylamino moiety on the scaffold.[79] Another class of pyrimidine–pyrazole hybrid compounds has been explored, and at least five compounds exhibited high inhibitory activity against CDK2/cyclin A2 ($IC_{50} < 20$ nmol/L). Among them, compound **11** was the most potent ($IC_{50} = 0.008 \pm 0.014$ μmol/L).[80]

The compounds with a 2,4-diaminopyrimidine scaffold showed comparable inhibitory potency against CDK2. These compounds were derived from NU6102, which replaced the 5-nitroso group with a 5-cyano-NNO-azoxy moiety, enriching the inhibitors' chemical diversity with 2,4-diaminopyrimidine scaffold.[81] Compound **12** (►**Fig. 9**), a benzamide derivative with a pyrimidine scaffold, targets CDK2 with an IC_{50} value of 45.8 ± 6.4 nmol/L. It inhibits the proliferation of triple-negative breast cancer cells, MDA-MB-468 cell line, in a time-dependent manner and induces S phase arrest and apoptotic cell death.[82] Compound **13** (►**Fig. 9**) has a 2-aminopyrimidine-fused azaindole scaffold and exhibits nanomolar inhibitory potency against CDK2/9. When **13** (2.5 mg/kg) was administered to the mice intravenously, it had a $t_{1/2}$ of 2.5 hours, an AUC of 437.1 ng/mL·h, an apparent volume of distribution (V_d) of 11.3 L/kg, and a plasma clearance (CL) of 3.1 L/h/kg. In contrast, an intraperitoneal injection of **13** (5.0 mg/kg) led to a $t_{1/2}$ of 4.4 hours, an AUC of 243.5 ng/mL·h, a V_d of 63.6 L/kg, and a CL of 0.9 L/h/kg. In the 4T1 mouse syngeneic model, compound **13** demonstrated significant dose-dependent tumor regression, achieving 90.58% tumor growth inhibition (TGI) at a dosage of 15 mg/kg

without any mortality. Notably, the body weights of the animals were not affected during the treatment.[83]

A novel class of compounds containing a pyrimidine scaffold has been discovered, with IC_{50} values in the micromolar range when the substituent at position 8 is of small size, up to the size of naphthyl or methoxyphenyl, as indicated by two-dimensional structure–activity relationships (SARs). However, the inhibitory activity of the inhibitors on other kinases has not been explored.[84] Compound **14** (►**Fig. 9**) is such a compound containing a benzothiazole ring structure. Molecular docking revealed the hydrogen bond interactions between the S atom on the benzothiazole ring and the residue Lys33, and the hydrogen bonding between the O and N atoms of the sulfonyl group and the residue Asp86. These interactions allow the compound to specifically target the CDK2/cyclin A2 complex and exhibit an IC_{50} value of 15.4 nmol/L. The potency of **14** is three times greater than AZD5438 (►**Table 2**), a positive control compound without the sulfonyl structural fragment, highlighting the advantages of the benzothiazole ring structure in the design of CDK2 inhibitor. Compound **14** also inhibits the proliferation of five human cancer cell lines (HCT116, MDA-MB-231, MCF-7, Hela, and PC-3 cells) with IC_{50} values of 0.70, 1.80, 10.91, 0.45, and 1.80 mmol/L, respectively. Further study indicated that **14** induces cell-cycle arrest and apoptosis in a dose-dependent manner.[85,86]

Modifications were performed through structure-based drug design and property space analysis, resulting in PF-06873600 (compound **15**, ►**Fig. 9**), a potential and selective candidate for tumor treatment, with K_i values for CDK2, CDK4, and CDK6 being 0.1, 1.2, and 0.1 nmol/L, respectively. Compound **15** has favorable spatial interactions with CDK2, with the 4-aminopiperidine sulfonamide moiety forming hydrophobic and polar interactions with important residues of CDK2. The (*1R,2R*)-2-hydroxy-2-methylcyclopentyl moiety enhances the lipophilic efficiency, occupying both the upper and lower lipophilic pockets and improving the effectiveness and stability of the compound. The methyl substituent fills the bottom lipophilic pocket effectively, while hydroxyl groups establish hydrogen bonds with Gln131 and a water molecule. The 6-difluoromethyl substituent interacts with the phenyl side chain of the gatekeeper residue Phe80 via van der Waals force. Those interactions produce potent and selective inhibitors of CDK2/4/6. Molecular dynamics simulations confirmed its better selectivity for CDK2 compared with CDK9. When **15** was orally administrated to mice and dogs, it had high absorption, with time to maximal absorption (T_{max}) being 0.25 and 1 hour, respectively. Compound **15** exhibited a CL of 63 mL/min/kg (CL), a V_d of 0.9 L/kg, and an oral bioavailability (F) of 13% in an NSG strain of mice, and a CL of 8.4 mL/min/kg, a V_d of 1.1 L/kg, and F of 59% in beagle dogs.[87] Furthermore, **15** inhibited cell activity and demonstrated antitumor activity in mice bearing an ovarian cancer cell line (OVCAR3) tumor. TGI studies have shown a 90% growth inhibition effect of **15** when it was orally dosed (50 mg/kg) as a single agent twice a day.[87]

The structures of other representative pyrimidine-based CDK2 inhibitors and their activity against CDKs are summarized in ►**Table 2**.[85,88–93]

Pyrazolo-Based CDK2 Inhibitors

FN-1501 (compound **16**, ►**Table 3**) is a derivative of 1-*H*-pyrazole-3-carboxamide with a pyrimidine-fused heterocyclic group at position 4 of the pyrazole. Its inhibitory activity against CDK2 was significantly increased ($IC_{50} = 2.47$ nmol/L) compared with the lead compound ($IC_{50} = 318$ nmol/L), suggesting that the substitution at position 4 of the pyrazole with a pyrimidine-heterocyclic group is the key moiety responsible for the inhibitory effect. The interaction between the moiety and gatekeeper Phe80 in the active site is primarily responsible for this effect (►**Fig. 10**). Compound **16** also demonstrated nanomolar inhibition of FLT3 ($IC_{50} = 0.27$ nmol/L), significant cytotoxicity agonists NCI60 cancer cell lines, and moderate metabolic stability in an *in vitro* liver microsome stability assay. **16** also exhibits tumor activity *in vivo*. In an MV4–11 xenotransplantation animal model, intravenous injection of **16** at a dosage of 30 and 40 mg/kg/day induces significant tumor regression. In addition, **16** were well tolerated and the experimental animals did not show any obvious signs of toxicity or body weight changes. Further study showed that a single intravenous administration of **16** or AT7519 into the ICR mice gave LD_{50} (median lethal dose) values of 185.67 and 32 mg/kg, respectively, suggesting a reduced toxicity of **16** compared with AT7519.[94]

Compound **17** (►**Fig. 10**) was derived from FN-1501, with greater inhibitory activity. The binding mode of **17** with CDK2 was elucidated using a docking model. In this mode, the aromatic ring occupies a hydrophobic pocket, the NH on the piperazine ring forms a hydrogen bond with Glu85 in the solvent region, and the five-membered ring on the pyrimidine-heterocyclic moiety extends into the ribose pocket.[95] When the piperazine ring, which extends into the solvent region, is removed, **18** was achieved with a 10-fold increase in potency against CDK2 and a more than 300-fold increase in selectivity relative to CDK4. The enhanced potency warrants further investigation.

Cheng et al reported dual-target compounds **19** and **20** based on a novel 1-*H*-pyrazole-3-carboxamide scaffold (►**Fig. 11**).[96] The compounds showed significant antiproliferative effects against five solid cancer cell lines, and remarkable inhibitory activity against CDK2 ($IC_{50} = 0.30$ and 0.56 nmol/L, respectively) and HDAC2 ($IC_{50} = 0.25$ and 0.24 nmol/L, respectively), suggesting their potential as potent therapeutic agents. The pharmacokinetic properties of **19** and **20** were investigated through intraperitoneally injecting **19** (20 mg/kg) and **20** (20 mg/kg) into ICR male mice. The data showed that **19** had a $t_{1/2}$ of 2.61 hours, a C_{max} of 7570 ng/mL, and an AUC of 30,700 ng/mL·h. However, **20** had a shorter $t_{1/2}$ of 1.63 hours, a C_{max} of 2170 ng/mL, and an AUC of 7200 ng/mL·h. In addition, **19** had a higher bioavailability ($F = 63.6\%$) compared with **20** ($F = 27.8\%$). When **19** (25 and 12.5 mg/kg) were intraperitoneally administered into the HCT116 xenograft nude mice

Table 2 The structures of pyrimidine-based CDK2 inhibitors

Compds.	Structure	IC_{50} (μmol/L) for CDKs	Ref.
AZD-5438	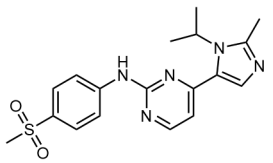	CDK1/cyclin B: 0.016 CDK2/cyclin A: 0.045 CDK2/cyclin E: 0.006 CDK4/cyclin D1: 0.449 CDK5/p25: 0.021 CDK7/cyclin H: 0.821 CDK9/cyclin T: 0.020	85
AUZ-454	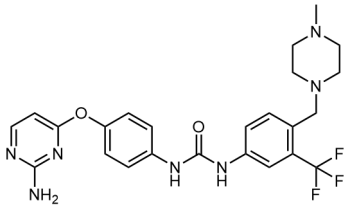	CDK2: 0.0082	88
Milciclib	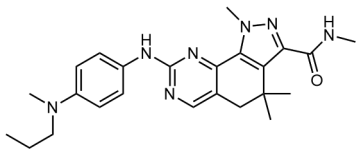	CDK1/cyclin B: 0.398 CDK2/cyclin A: 0.045 CDK2/cyclin E: 0.363 CDK4/cyclin D1: 0.160 CDK5/p35: 0.265 CDK7/cyclin H: 0.150	89
SB1317 (TG02)	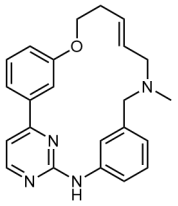	CDK2: 0.013	90
Roniciclib	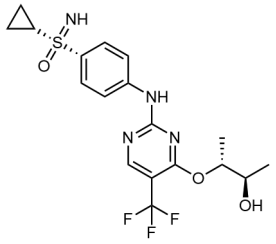	CDK1/cyclin B: 0.007 CDK2/cyclin E: 0.009 CDK4/cyclin D: 0.011 CDK7/cyclin H: 0.025 CDK9/cyclin T1: 0.005	91
NU6140	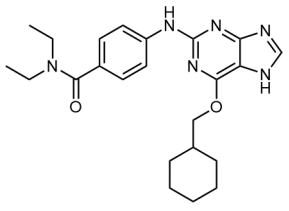	CDK1/cyclin B: 6.6 CDK2/cyclin A: 0.41 CDK4/cyclin D: 5.5 CDK5/p25: 15 CDK7/cyclin H: 3.9	92
R547	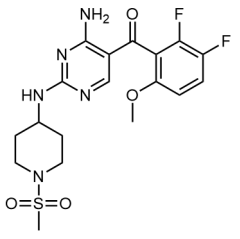	CDK1: 0.001 CDK2: 0.003 CDK4: 0.001	93

models once daily, tumor growth was significantly inhibited, with TGIs of 37.0 and 51.0%, respectively, and no apparent weight changes or signs of toxicity were observed in animals, suggesting an *in vivo* antitumor activity of the compound.[96]

Compound **21** (►**Fig. 11**) is a pyrazolo[1,5-*a*][1,3,5]triazine derivative that targets CDK2. Molecular docking models indicate that pyrazole N and H atoms of **21** form two hydrogen bonds with the hinge region, resulting in an IC_{50}

Table 3 The structures of pyrazolo-based CDK2 inhibitors

Compds.	Structure	IC_{50} (μmol/L) for CDKs	Ref.
FN-1501	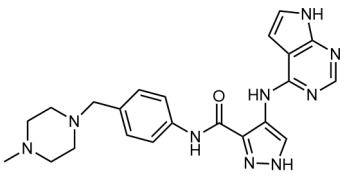	CDK2/cyclin A: 0.00247 CDK4/cyclin D1: 0.00085 CDK6/cyclin D1: 0.00196	94
CT7001	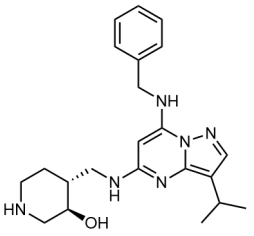	CDK1: 1.8 CDK2: 0.62 CDK4: 49 CDK5: 9.4 CDK6: 34 CDK7: 0.04 CDK9: 1.2	104
AT7519	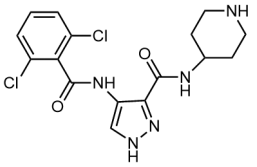	CDK1/cyclin B: 0.21 CDK2/cyclin A: 0.047 CDK3/cyclin E: 0.360 CDK4/cyclin D1: 0.100 CDK5/p35: 0.013 CDK6/cyclin D3: 0.170 CDK7/cyclin H: 2.4 CDK9/cyclin T: < 0.01	105
FMF-04–159–2	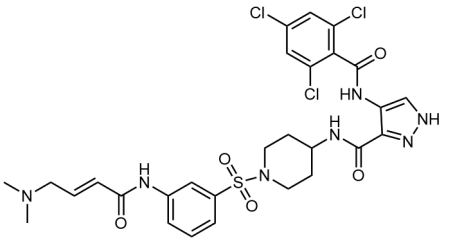	CDK1: 0.054 CDK2: 0.095 CDK4: 0.021 CDK5: 0.041 CDK6: 0.0034 CDK9: 0.029 CDK10: 0.077 CDK12: 0.014 CDK14: 0.094	106
NVP-LCQ195	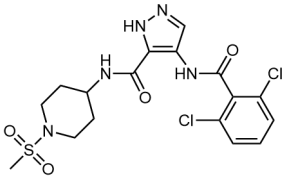	CDK1/cyclin B: 0.002 CDK2/cyclin A: 0.002 CDK2/cyclin H: 0.005 CDK3/cyclin E: 0.042 CDK5/p25: 0.001 CDK5/p35: 0.001 CDK6/cyclin D3: 0.187 CDK7/cyclin H: 3.564 CDK9/cyclin T1: 0.015	107
BMS-265246	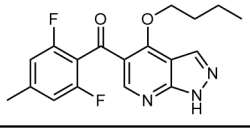	CDK1/cyclin B: 0.006 CDK2/cyclin E: 0.009 CDK4/cyclin D: 0.230	108
PHA-793887	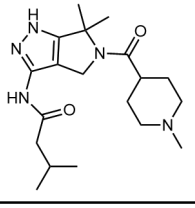	CDK1/cyclin B: 0.060 CDK2/cyclin A: 0.008 CDK2/cyclin E: 0.008 CDK4/cyclin D1: 0.062 CDK5/p25: 0.005 CDK7/cyclin H: 0.010 CDK9/cyclin T1: 0.138	109

value of 1.85 μmol/L. Compound **21** exhibited the highest inhibitory effect on cell growth, with an average inhibition rate of 41.77% in a study that screened the antiproliferation activity of a series of novel pyrazolo[1,5-*a*][1,3,5]triazine derivatives on 60 cancer cell lines. It is also observed that **21** can adapt well to deep hydrophobic pockets when a halogen atom is possessed.[97]

HSD992 (compound **22**, ►**Fig. 11**), which possesses a novel tetrahydro-3*H*-pyrazolo[4,3-*a*]phenanthridine core-based scaffold, exhibits significant inhibitory activity against

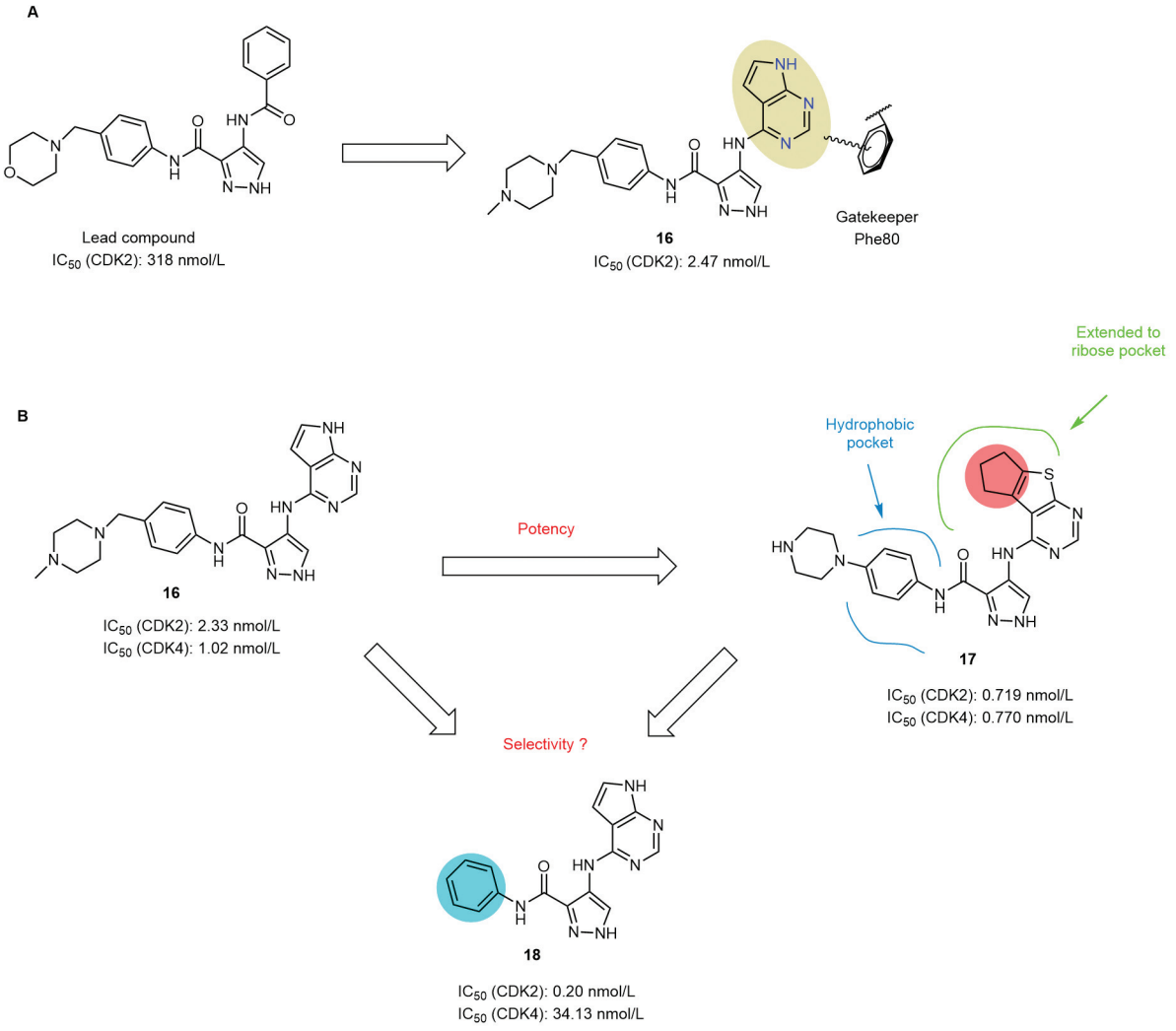

Fig. 10 (A) Key moiety for inhibitory activity of **16**. (B) Optimization of **16**.

CDK2 and CDK3, with IC_{50} values of 57 and 18 nmol/L, respectively. Additionally, it demonstrates moderate inhibition against CDK9, while no inhibitory effects on other CDKs including CDK1 and CDK4/6. Compound **22** inhibited the proliferation of cancer cells, including lymphoma cell lines, lung cancer cell lines, and cervical cancer cell lines at a concentration of 1 µmol/L, and is particularly effective against lung cancer cell lines. **22** inhibited NCI-520 cells with an IC_{50} value of 307 nmol/L.[98]

More efforts have been focused on the development of potent and selective CDK2 inhibitors including PF-06873600 and PF-07104091 from Pfizer, BLU-222 from Blueprint Medicines, INX-315 from Incyclix Bio., and INCB123667 from Incyte.[99–102] PF-07104091 (compound **23**, ►**Fig. 11**), an orally available CDK2 inhibitor, is being investigated for its potential antitumor activity in advanced or metastatic solid tumors. **23** dose-dependently inhibited tumor growth in a human ovarian cancer cell model and demonstrated synergistic effects when administered concurrently with the first-line drug palbociclib in a breast cancer cell model.[103]

The structures of other representative pyrazolo-based CDK2 inhibitors and their activity against CDKs are summarized in ►**Table 3**.[94,104–109]

Pyridine-Based CDK2 inhibitors

Compound **24** (►**Fig. 12**) with a pyridine scaffold was designed and synthesized using a scaffold hopping approach. It showed optimal inhibitory activity against cancer cell lines H522 ($IC_{50} = 2.89$ µmol/L) and U87 ($IC_{50} = 3.19$ µmol/L). However, its inhibitory activity against CDK2 only reaches the micromolar level, with an IC_{50} value of 1.8 ± 0.5 µmol/L.[110]

Wu et al developed a set of CDK2 inhibitors based on the structure of CYC202 using imidazo[4,5-*c*]pyridine as a core scaffold.[111] Among them, compound **25** (►**Fig. 12**) achieved nanomolar inhibitory activity against CDK2, with an IC_{50} value of 21 nmol/L, and demonstrated potential antiproliferation effects against three different cancer cell lines with the IC_{50} values at the micromolar range (IC_{50} values of 3.71, 3.85, and 1.56 µmol/L for HL60, A549, and HCT116 cells, respectively). Molecular docking and dynamic study

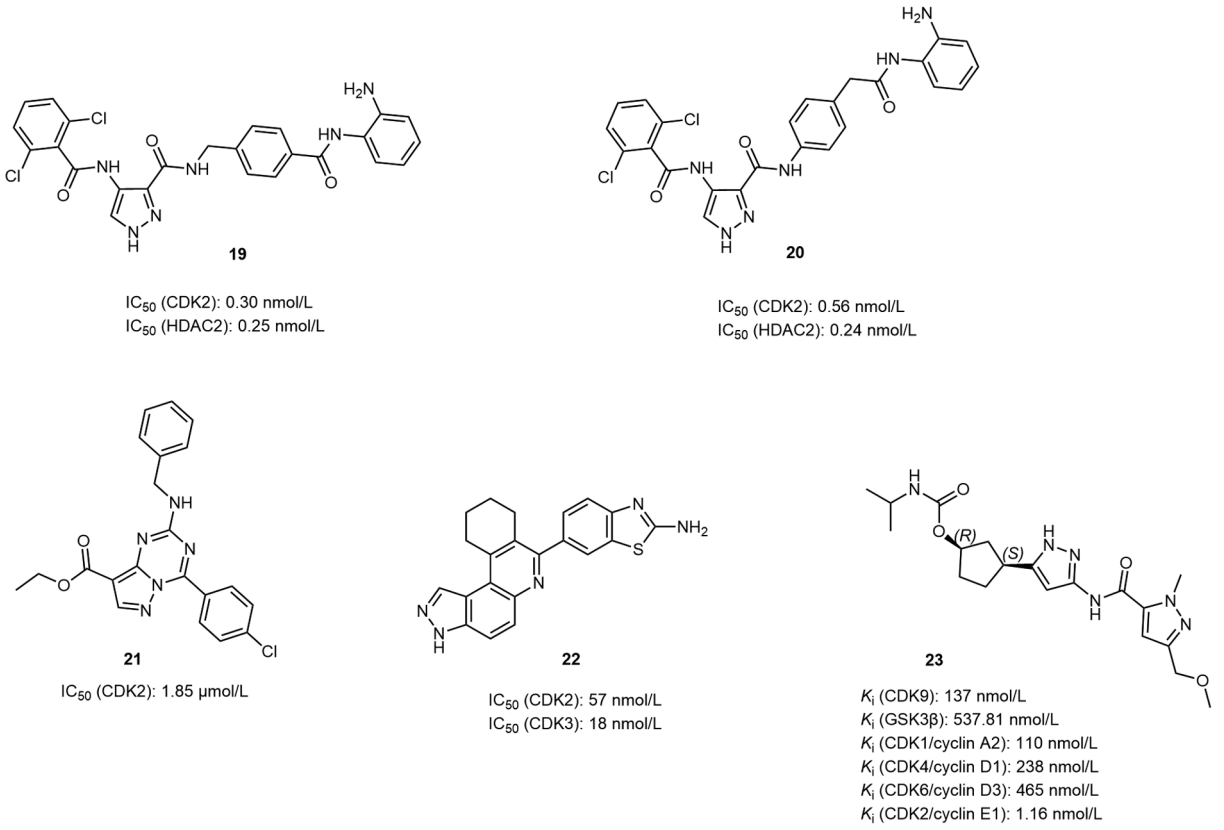

Fig. 11 The structures of compounds **19**–**23**.

techniques identified pyridine-3-ylmethyl moiety as a highly promising pharmacophore in advancing novel CDK2 inhibitors in the future.[111]

Other Novel Scaffolds

IIIM-290 (compound **26**; ►**Fig. 13**), which has a rohitukine scaffold, is the first orally bioavailable CDK inhibitor, acting as a dual-target inhibitor of CDK2/9, with IC_{50} values of 16 ± 1 and 1.9 ± 1 nmol/L, respectively. Compound **26** exhibits anticancer activity in cell and animal models. Compound **26** inhibited the proliferation of HL-60 and MIAPaCa-2 cells with GI_{50} values of 0.9 and 1 μmol/L, respectively. The pharmacokinetic properties of **26** were assessed in BALB/c mice. The results showed that oral administration of **26** at a dosage of 10 mg/kg had a $t_{1/2}$ of 4.65 hours and an AUC of 4,503 nmol/L·h, and intravenous injection of **26** at a dosage of 1.0 mg/kg had a $t_{1/2}$ of 5.46 hours and a CL of approximately 55 mL/min/kg. Compound **26** achieved a 71% absolute oral bioavailability and good tissue distribution in various organs including the pancreas, lungs, liver, and kidneys. By oral administration, **26** caused 31 and 39% TGI at dosages of 70 and 100 mg/kg, respectively, without causing animal death. The oral MTD in mice for **26** is 100 mg/kg. The compound showed promising TGI in three human xenograft models, including pancreatic cancer, colon cancer, and leukemia cancer. The compound has also a stable metabolism, no CYP/efflux pump responsibility, no mutagenicity/genotoxicity or cardiotoxicity, and exhibits good characteristics in acute oral toxicity in rats.[112]

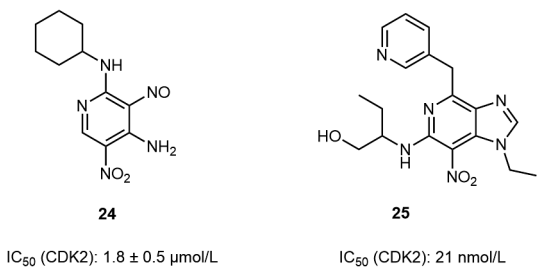

Fig. 12 The structures of compounds **24** and **25**.

Compound **27** (►**Fig. 13**), a 5,6-dihydropyrimido[4,5-*f*] quinazoline derivative with a quinazoline moiety, showed potent inhibitory activity toward CDK2 with an IC_{50} value of 0.09 μmol/L, and antiproliferative activity against MCF-7 cells ($IC_{50} = 1.1 \pm 0.1$ μmol/L) and HCT116 cells ($IC_{50} = 1.4 \pm 0.2$ μmol/L).[113]

In 2017, Arba et al performed an *in silico* study of a set of porphyrin–anthraquinone hybrids with meso-substituents, specifically pyridine or pyrazole rings. Molecular docking analysis suggested that all compounds target the ATP-binding site of CDK2.[114] A new class of thiazol–hydrazono–coumarin hybrid scaffold compounds inhibited CDK2/cyclin E complex, with IC_{50} values ranging from 0.022 to 1.629 nmol/L. Besides, compound **28** upregulated CDK2 regulators, p21 and p27, with 2.3- and 5.7-fold increases, respectively, and inhibited the proliferation of the HeLa cell line with an IC_{50} value of 0.0596 μmol/L.[115] Compound **29** (►**Fig. 13**), an

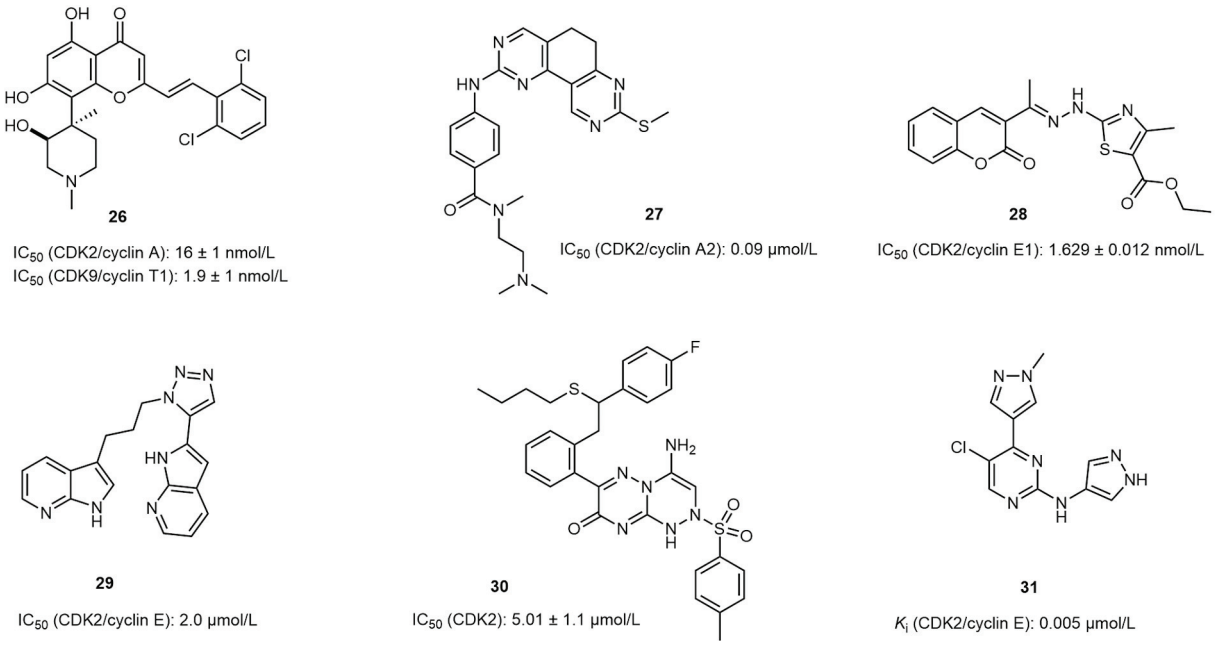

Fig. 13 The structures of compounds **26–31**.

azaindole–triazole hybrid scaffold analog, exhibits an IC_{50} value of 2 μmol/L against CDK2/cyclin E.[116] The pyrazolo-4-thiophen-thiazepinone scaffold compounds, targeting CDK2, form three hydrogen bonds with the hinge region, with IC_{50} values ranging from 3.9 to 10.3 μmol/L.[117] A series of fluorine-substituted amino-1,2,4-triazino[4,3-*b*]-1,2,4-triazino-8-ones compounds have been synthesized to enhance the bioavailability, and compound **30** (►**Fig. 13**) demonstrated the best potency ($IC_{50} = 5.01$ μmol/L).[118]

Fanta et al synthesized a series of *N*,4-di(1*H*-pyrazol-4-yl) pyrimidin-2-amine derivatives through the substitution of the phenylsulfonamide moiety with pyrazole-derived groups to enhance the efficiency and specificity of the lead compound.[119,120] Among those compounds, compound **31** (►**Fig. 13**) exhibited the highest potency as a CDK2 inhibitor, with a K_i value of 0.005 μmol/L. It showed a certain degree of selectivity toward other CDKs and demonstrated submicromolar antiproliferative activity against 13 cancer cell lines ($GI_{50} = 0.127$–0.560 μmol/L). Docking analysis showed that **31** may establish two hydrogen bonds with Leu83 located in the hinge region of the ATP-binding pocket. Additionally, the 2-amino group of the pyrimidinyl-N1 will likely form a second hydrogen bond with the NH group of the corresponding amino acid residue.[120] Some representative CDK2 inhibitors with other novel scaffolds since 2015 are shown in ►**Table 4**.[75,81,84,111,115,116,121]

Type II Inhibitors

The conformational changes of CDK2, particularly in the DFG motifs involved in ATP binding, occur as it transitions between the active and inactive states. Type II inhibitors selectively target the inactive conformation of CDK2 by inducing an outward flip of the conserved tripeptide motif DFG, known as the DFG-out conformation. These inhibitors bind to free CDK2, stabilizing its inactive conformation and preventing activation by cyclin. The first co-crystal structure of CDK2 with a type II inhibitor K03861 (**32**) was reported in 2015 (►**Fig. 14**). Analysis of this inhibitor reveals that two key groups, the "head" hinge-binding moiety (aminopyrimidine ring) and the hydrogen-bonding moiety (urea moiety), play a crucial role in stabilizing the conformation of the T-loop and establishing hydrogen bonds with the hinge region, αC-helix, and DFG motif.[53,88]

Type III and IV Inhibitors (Allosteric Inhibitors)

The ATP-binding pockets show a high degree of conservation among the 518 members of the human protein kinome, which challenges the selectivity of ATP-competitive inhibitors such as GW8510, SU9516, CVT313, etc., which often lack specificity.[8,55] In contrast, allosteric sites exhibit greater variability. Residues within these sites are less conserved among the kinases. This leads to the allosteric inhibitors targeting the residues with higher selectivity, reduced toxicity, and longer drug–target residence time.[122,123]

Type III Inhibitors

In 2011, Betzi et al used 8-anilino-1-naphthalene sulfonate (ANS) to discover a novel binding site for CDK2. The compound interferes with the binding of CDK2 to cyclin A and binds to a hydrophobic pocket adjacent to the ATP-binding site, formed by the αC-helix and the nearby β3–β5 strands of the N-terminal lobe. Co-crystal structure analysis reveals the spacious nature of this pocket, capable of accommodating two ANS compounds that extend from the DFG region above the αC-helix.[1]

Upon cyclin A binding to CDK2, the αC-helix undergoes a conformational change, narrowing the large hydrophobic pocket in free CDK2. When ANS binds to this hydrophobic pocket, it stabilizes CDK2 in a conformation that is unable to interact with cyclins.[1,124] In ANS-bound CDK2

Table 4 Other novel scaffolds since 2015

Scaffold	Structure	Representative compds.	IC_{50} (μmol/L) for CDKs	Ref.
Pyrazolo[3,4-*d*]pyrimidines	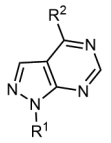	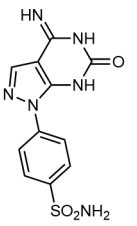	CDK2: 0.19	75
2,4-Diaminopyrimidine	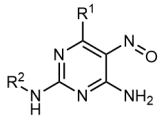	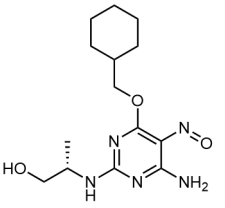	CDK2: 0.16	81
Imidazo[1,2-*c*]pyrimidine-5(6*H*)-one	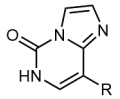	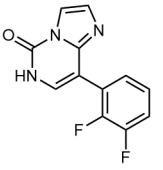	CDK2/cyclin E: 1.3	84
3*H*-Imidazole[4,5-*c*]pyridine	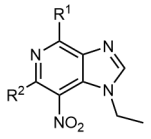	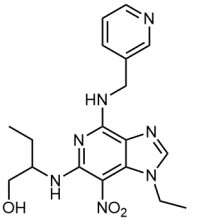	CDK2: 0.021	111
Thiazol-hydrazono-coumarin hybrid	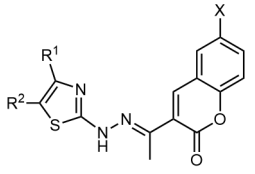	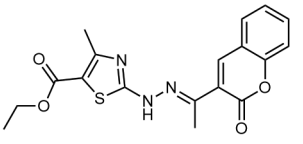	CDK2/cyclin E1: 0.0016	115
N^2,N^4-Disubstituted pyrimidine-2,4-diamines	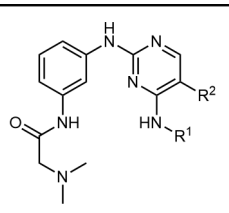	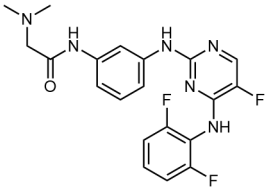	CDK2/cyclin A: 0.083 CDK9/cyclin T1: 0.10	121
7-Azaindole-based tri-heterocyclic	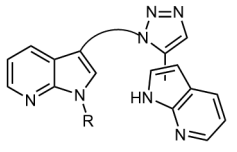	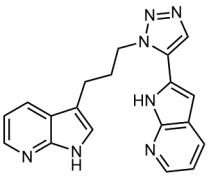	CDK2/cyclin E: 2.0	116

conformations (PDB:3PXF), the inner compound (ANS1) forms three hydrogen bonds with the polar head of Lys33, the NH groups of Asp145 and Phe146 in the DFG motif, and π–π interactions with Tyr15 and Phe80 (gatekeeper). The outer compound (ANS2) forms two hydrogen bonds with the polar head of Lys56 and the NH group of His71 through the oxygen atom on its sulfonic acid group.[125]

To disrupt protein–protein interactions (PPIs), Rastelli et al identified seven ligands as first-in-class allosteric inhibitors of CDK2, through a crystal structure of CDK2 with an

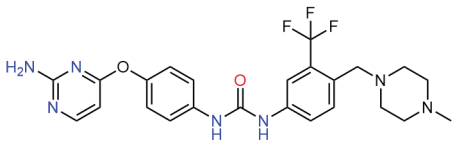

32

Fig. 14 The structure of compound **32**.

open allosteric pocket. Although these ligands showed high or similar affinity for CDK2, with EC_{50} values in the micromolar range, they did not exhibit significant inhibitory activity against the CDK2/cyclin A complex. This suggests that in the active conformation of CDK2/cyclin A, structural changes in CDK2 result in the obligatory closure of the ANS allosteric site, rendering it inaccessible to ligands.[126] In the same year, short peptides targeting a noncatalytic pocket near the CDK2/cyclin interface were reported to weaken the formation of CDK2/cyclin E1 complex through allosteric interactions. However, peptide inhibitors have poor oral bioavailability.[127]

In 2015, Hu et al discovered a nonpeptide allosteric inhibitor, B2 (compound **33**, ►**Fig. 15**), that disrupted the interaction between CDK2 and cyclin A3. Compound **33** showed potent inhibitory activity against CDK2/cyclin A3, with an IC_{50} value of 52.12 ± 1.35 μmol/L, in a concentration-dependent trend,[128] and inhibited the proliferative activity of A549, HepG2, and MDA-MB-231 cell lines, with IC_{50} values of 85.24, 299.7, and 460.4 μmol/L, respectively.

Carlino et al used compound **34** (a hexahydrocyclopenta[*c*]quinoline derivative) as the probe to explore the chemical and biological features of the allosteric pocket and synthesized the enantiomers of compound **35** (►**Fig. 15**), confirming that they are type III inhibitors.[125] They further investigated the SARs of CDK2 type III inhibitors, using hexahydrocyclopenta[*c*]quinolone as a scaffold. The study confirmed the key role of carboxylic acid and nitro groups in inhibiting CDK2. These groups formed a salt bridge with the polar head of the conserved Lys33 residue and hydrogen bonds with the backbone NHs of the Asp145 and Phe146 residues in the DFG motif.[129]

Type IV Inhibitors

Craven et al used a quantitative irreversible tethering approach to identify CDK2-selective allosteric (type IV) inhibitors **36**–**38** (►**Fig. 15**), which contained an acrylamide moiety covalently bound to the Cys177 residue of CDK2. The selectivity of these inhibitors may be attributed to the presence of a cysteine residue at an equivalent position to Cys177 only in CDK2.[130]

Other Allosteric Inhibitors

Pellerano et al discovered a novel allosteric site on CDK2 near the T-loop and the interface of the CDK2/cyclin A complex.[55] They identified a new category of CDK2 inhibitors, referred to as MMQs, which shared a pentacyclic quinacridine scaffold. Among the inhibitors, MMQ3 (compound **39**, ►**Fig. 16**) exhibited the highest potency, as indicated by its lowest EC_{50} (25 μmol/L) against CDK2/cyclin A and submicromolar IC_{50} values against a large panel of different cell lines, including breast, lung, prostate, and colon cancer. Compound **39** was found to extend across the T-loop of CDK2 and establish interactions with crucial residues such as Cys177 and Glu208, with Cys177 exhibiting heightened sensitivity to binding with **39**.[55] In contrast to the previous four binding modes, this particular binding mode interferes with the T-loop conformational switch in CDK2 by specifically targeting the T-loop and blocking the substrate-binding site, thereby inhibiting substrate phosphorylation.

P27 (compound **40**, ►**Fig. 16**), an endogenous short peptide, is a negative regulator that inhibits the phosphorylation of the CDK2/cyclin A complex. The binding site of **40** is located in the cyclin-binding groove (CBG) on cyclin A, and it specifically recognizes the Leu-Phe-Gly (LFG) motif region of **40**. A study used this specific fragment to design a series of

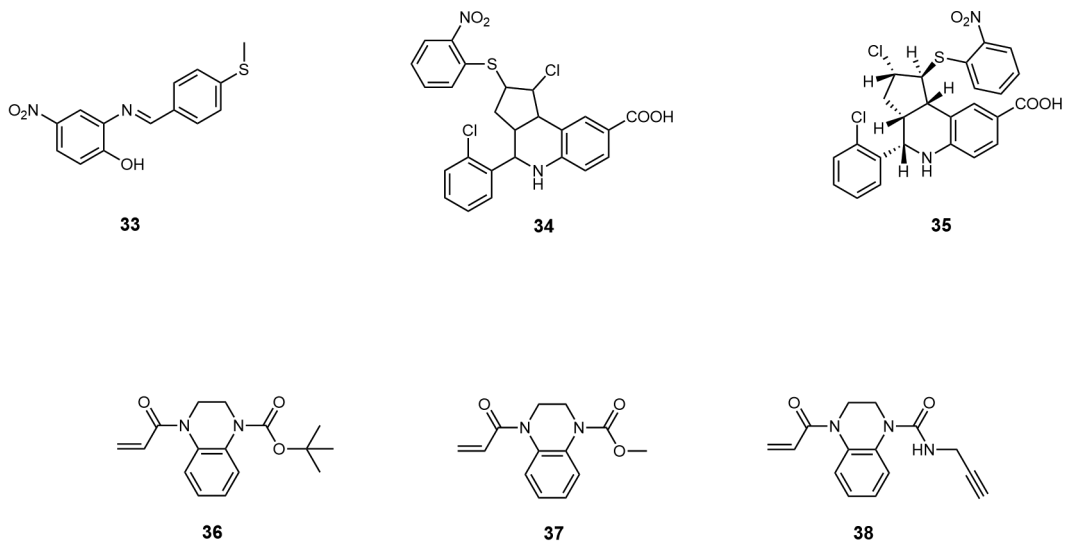

33 34 35

36 37 38

Fig. 15 The structures of type III CDK2 inhibitors (**33**–**35**) and type IV inhibitors (**36**–**38**).

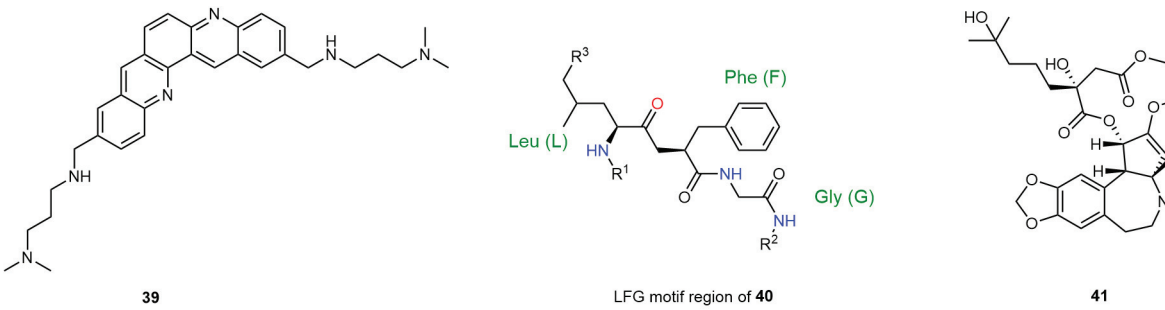

Fig. 16 The structures of compounds **39–41**.

peptidomimetics and analytical methods such as ADME (absorption, distribution, metabolism, excretion) evaluation, and electrostatic potential mapping were employed to determine the optimal substituent at the phenyl ring position.[131] The results suggested that a smaller substituent is more suitable for interaction with residues located at the active site of cyclin A.

In 2016, Premnath et al synthesized a class of benzoic acid scaffold derivatives that target CBG on cyclin. Benzamide-capped peptidomimetics exert inhibitory effects by mimicking the function of key peptide determinants and competing with substrate binding.[132] Another novel targeting site involves disruption of PPI between CDC25B and CDK2/cyclin A, as demonstrated by molecular dynamics simulation and MM/PBSA.[133] Subsequently, in 2017, a novel allosteric site in CDK2 was predicted using the AllositePro method, which combines pocket feature and perturbation analysis to predict allosteric sites in proteins. The crystal structure revealed that two key residues in the allosteric pocket are Arg150 and Tyr180. This approach provides a new strategy for the discovery of allosteric sites in CDK2 and contributes to the design of selective CDK2 inhibitors with novel scaffolds.[134]

In 2022, Zhang et al identified two additional drug-binding sites at the PPI interface between CDK2 and cyclin A. Homoharringtonine (compound **41**, ►**Fig. 16**) exhibited significant affinity for PPI and is effective in disrupting the binding of cyclin A and CDK2. Compound **41** formed three hydrogen bonds with Thr47, Arg50, and Arg150 in CDK2, thereby obstructing the interaction between CDK2 and cyclin A while promoting the interaction between CDK2 and tripartite motif 21 (Trim21). This interaction with Trim21 triggered the autophagy mechanisms, leading to the degradation of CDK2 in cancer cells.[135]

CDK2 PROTAC

Proteolysis-targeting chimeras (PROTACs) offer a promising alternative to targeted therapy, characterized by superior potency, selectivity, and reduced drug resistance compared with traditional CDK small-molecule inhibitors. A typical PROTAC molecule consists of three main components: a ligand that binds to the target protein of interest, a ligand that recruits the E3 ubiquitin ligase, and an appropriate linker connecting these two ligands. PROTACs form ternary complexes by simultaneously engaging with target proteins and E3 ligases. Importantly, PROTACs can effectively target "undruggable" proteins that lack accommodating inhibitor-binding sites and can overcome drug resistance issues caused by small-molecule inhibitors leading to overexpression of pathogenic proteins. Furthermore, PROTACs do not require high affinity and concentration like small-molecule inhibitors, and their catalytic role in mediating protein degradation helps circumvent potential side effects.[136,137]

In 2019, Zhou et al conducted a study on the discovery of innovative CDK small-molecule PROTAC degraders.[138] A9 (**42**) based on AT-7519 and F3 (**43**) based on FN-1501 were identified as the most potent CDK2-selective degraders and CDK2/CDK9 dual degraders, respectively (►**Fig. 17**). Compound **42** exhibits modest antiproliferative activity in PC-3 cells with an IC_{50} value of 0.84 μmol/L, while **43** achieved an IC_{50} value of 0.12 μmol/L. Compound **43** induced approximately 50% degradation of CDK2 and CDK9 at concentrations of 62 and 33 nmol/L, respectively. The structure of **42** involves connecting a pan CDK inhibitor AT-7519 to a cereblon (CRBN) ligand via a linker. Mechanistic studies suggested that **42**-induced degradation of CDK2 depends on CDK2, CRBN, and the proteasome. This study represents an initial step toward developing more effective CDK2-selective degraders, with the potential for therapeutic applications in human prostate cancer and other conditions through further structural modification, mechanism study, and safety evaluation.[138]

The degradation of CDK2 may represent a therapeutic strategy in certain cancers characterized by CCNE1 overexpression, such as ovarian cancer. Teng et al reported CRBN-recruiting PROTAC TMX-2172 (compound **44**, ►**Fig. 17**), a selective CDK2/CDK5 dual degrader.[139] Compound **44** exhibits a high degree of selectivity for the degradation of CDK2 and CDK5, surpassing its effect on other cell-cycle CDKs and transcriptional CDKs. Compound **44** induced CDK2 degradation at a concentration of 250 nmol/L and also resulted in CDK5 degradation in Jurkat cells. Treatment with **44** in OVCAR8 cells showed a dose-dependent degradation of CDK2 and CDK5. Furthermore, **44** exhibited more potent antiproliferative activity ($GR_{50} = 33.1$ nmol/L) in OVCAR8 cells than the negative control ZXH-7035. Importantly, even though **44** degraded CDK5, the deletion of CDK5 achieved through genome-wide CRISPR screening and shRNA-knockdown did not impede the growth of OVCAR8 cells. This suggests that the primary mechanism by which **44** exerts its antiproliferative effects in OVCAR8 cells is through

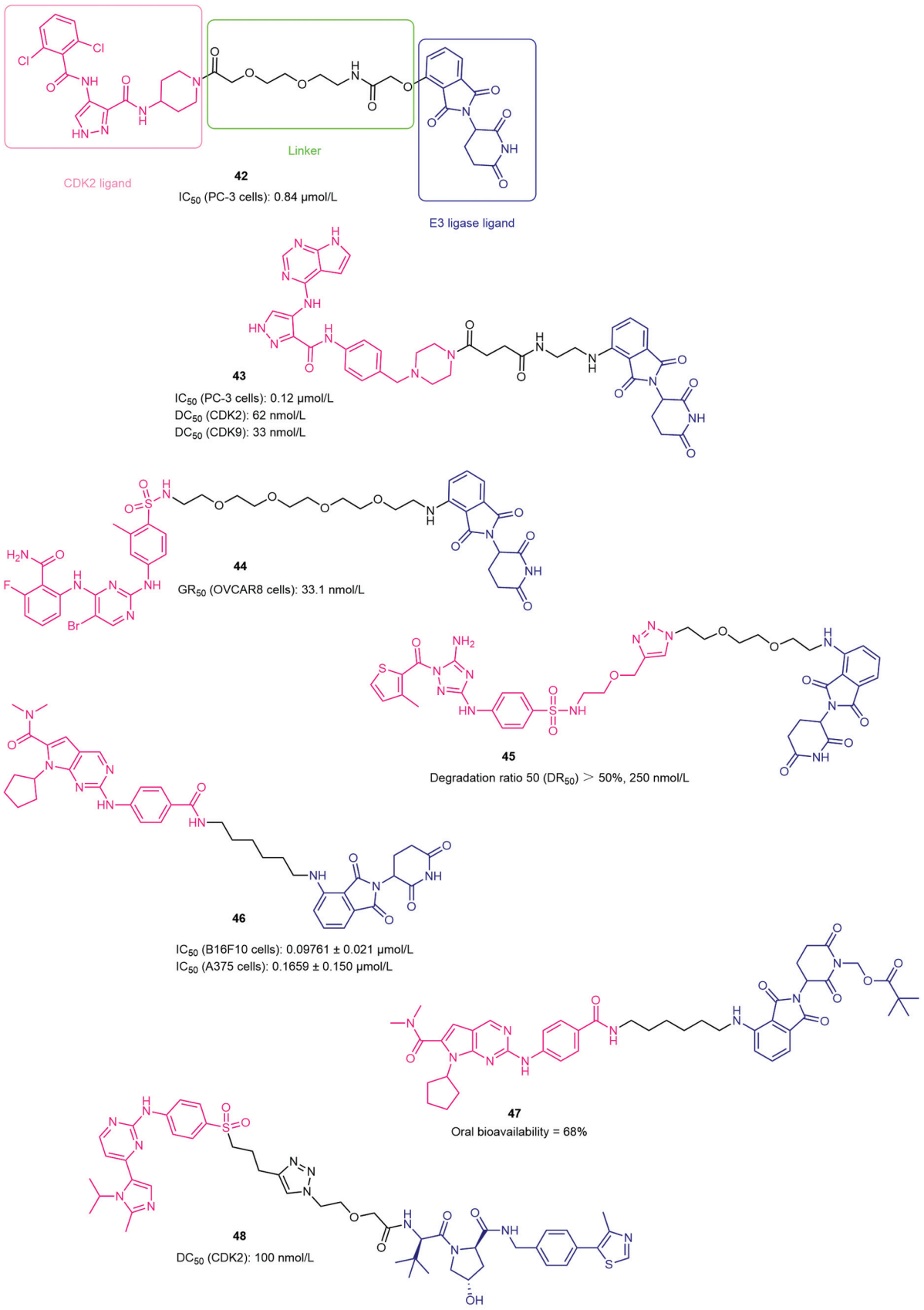

Fig. 17 The structures of reported selective CDK2 proteolysis-targeting chimerics.

the degradation of CDK2, highlighting its therapeutic benefits in the potential treatment of ovarian cancer.

Wang et al identified CPS2 (compound **45**, ►**Fig. 17**) as a selective CDK2 degrader with an exceptional safety profile. They conducted a series of experiments to evaluate the ability of **45** to induce CDK2 degradation in various cell lines, assess the degradation selectivity of the compound, confirm its selectivity in cells, and perform related safety evaluations.[140] After 3 days of treatment with **45**, there was no significant change in the relative growth rate of the normal cell line (Beas-2b cells) and the engineered cell line (293T cells). In addition, the outcomes of the acute toxicity experiment by intraperitoneal injection of a large amount of **45** into mice showed that when using **45** at a dose of 400 mg/kg on the first day, there were no apparent toxic reactions or deaths within 1 week and the body weights of animals exhibited an upward trend. Compound **45** effectively blocked tumor cell growth without substantially inducing cell death. The treatment with **45** at 250 nmol/L for 2 hours is sufficient to reduce CDK2 by more than 50% in NB4 and Ramos cells. Compound **45** resulted in cell differentiation through the reduction of CDK2 levels, leading to the upregulation of CD11b (a recognized marker of acute myeloid leukemia [AML] differentiation) in various AML cell lines, including NB4, U937, and HL60 cells. Moreover, **45** induced notable changes in nuclear morphology and enhanced nitroblue tetrazolium reduction. These findings suggested that **45** has the potential to induce on-target myeloid differentiation in AML cells. In addition, **45** significantly promoted the differentiation of primary AML cells by degradation of CDK2. RNA-sequencing experiments demonstrated that **45** significantly influenced the transcription of genes associated with cell differentiation and maturation pathways, which are essential for AML cell differentiation. **45** also has the potential to treat diseases caused by nonenzymatic activity of CDK2.

A novel compound **46** (►**Fig. 17**), obtained by conjugating a Ribociclib derivative and Pomalidomide through a linker, could effectively degrade CDK2/4/6 in various cancer cells and downregulate the phosphorylation of Rb. Compound **46** demonstrated significant antiproliferative activity against a wide range of human cancer cell lines, particularly in melanomas ($IC_{50} = 0.09761 \pm 0.021$ μmol/L in B16F10 cells; $IC_{50} = 0.1659 \pm 0.150$ μmol/L in A375 cells). Western blot analysis suggested **46** induced caspase-dependent apoptosis in melanoma cells via the P53/Bcl-2/Bax apoptotic pathway.[141] Additionally, Wang et al addressed the issue of poor oral bioavailability of PROTAC molecules with CRBN ligands by developing the orally bioavailable prodrug **47**. The preliminary pharmacokinetic analysis revealed that orally administered **46** at a dosage of 200 mg/kg resulted in a C_{max} of 692,268 ng/mL, T_{max} (time to reach C_{max}) of 0.25 hours, and AUC_{0-12} (area under the concentration–time curve from 0 to 12 hours) of 82,280.39667 ng/mL; and orally administered **47** at a dosage of 200 mg/kg resulted in a C_{max} of 2,261,897 ng/mL, a T_{max} of 0.25 hours, and an AUC_{0-12} of 2,810,197.617 ng/mL. The prodrug exhibited high oral bioavailability of up to 68%. Compound **47**, via oral administration, not only demonstrated favorable pharmacokinetic characteristics but also suppressed the proliferation of B16F10 tumors and induced the degradation of CDK2/4/6. The development of **47** offers a potential solution for the oral delivery of PROTAC molecules by incorporating a lipophilic group onto CRBN ligands.

Hati et al identified PROTAC-8 (compound **48**, ►**Fig. 17**), an AZD5438-based PROTAC, as a selective CDK2 degrader that could protect against cisplatin- and noise-induced hearing loss.[142] Compound **48**, synthesized by conjugating AZD5438 with an E3 ligase ligand VH-032 using a linker, exhibited selective and partial degradation of CDK2. Compound **48** at 100 nmol/L resulted in approximately 50% degradation of CDK2 in HEI-OC1 cells. Importantly, **48** exhibited selectivity for degradation of CDK2 over CDK1, CDK5, CDK7, and CDK9. Molecular dynamics simulations and *in vivo* zebrafish models provided insights into the structural and functional foundations of **48** as a CDK2-specific degrader, highlighting its therapeutic potential in treating hearing loss and various types of cancers.

CDK2 Inhibitors in Clinical Trials

Several CDK2 inhibitors are currently in clinical development as anticancer drugs (►**Table 5**). Prior to this, many inhibitors were discontinued from clinical development due to off-target effects, associated side effects, and failure to achieve acceptable clinical endpoints.[20] Flavopiridol (Alvocidib) is a flavone alkaloid inhibitor and the first CDK inhibitor to enter clinical trials, while R-roscovitine (Seliciclib, CYC202) is a purine analog. Both are pan-CDK inhibitors and have exhibited unsatisfactory outcomes in previous clinical trials. Currently, they are being utilized in combination with other anticancer drugs in phase I and phase II clinical trials.[20] The clinical research progress of dinaciclib is noteworthy, encompassing a broad spectrum of solid tumors and hematological malignancies. Phase III clinical trials focusing on chronic lymphocytic leukemia (CLL) have revealed that dinaciclib demonstrates promising anticancer activity and tolerability in patients with refractory CLL, particularly when compared with ofatumumab, a targeted anti-CD20 monoclonal antibody. The prospect of combining dinaciclib with other novel therapies is highly anticipated.[143] Furthermore, PF-07104091, a selective CDK2 inhibitor, is currently under investigation as a single treatment and in combination with other therapies for small cell lung cancer, ovarian cancer, and breast cancer. Additionally, it is being studied in combination with PF-06873600 for the treatment of breast cancer and solid tumors. These clinical trials are presently recruiting participants and are in the phase I/II stage of drug development. The emergence of CDK2/4/6 inhibitors in recent years has been prominent in the treatment of breast cancer and ovarian cancer. This trend underscores the potential of CDK2 inhibitors to address drug resistance challenges associated with CDK4/6 inhibitors in breast cancer.[144] The phase II clinical trials for the CDK2/4/6 inhibitor PF-06873600 are currently ongoing in patients with hormone receptor-positive (HR+) and human epidermal growth factor receptor 2 negative (HER2-) metastatic breast cancer. Additionally, several other compounds targeting CDK2 are at

Table 5 CDK2 inhibitors in clinical trials

Drug	Classification	Stage	Indication
Flavopiridol (Alvocidib)	Pan-CDK	Phase I Phase II	Relapsed/refractory acute myeloid leukemia
		Phase I/II	MDS
		Phase I	Newly diagnosed AML
		Phase I Phase II	AML
R-roscovitine (Seliciclib, CYC202)	Pan-CDK	Phase I	Advanced solid tumors
		Phase II	Cushing disease
TG02 (Zotiraciclib, SB1317)	Pan-CDK	Phase I	Advanced hepatocellular carcinoma
		Phase I	Recurrent/progressive high-grade gliomas
		Phase I	Elderly newly diagnosed or adult Relapsed patients with anaplastic astrocytoma or glioblastoma
		Phase I	Locally advanced primary and recurrent oncogenic RAS exon 2 mutant colorectal cancer
		Phase I/II	Recurrent anaplastic astrocytoma and glioblastoma
		Phase I/II	Recurrent high-grade gliomas with IDH1 or IDH2 mutations
AT7519 (AT7519M)	Pan-CDK	Phase I	Solid tumors that are metastatic or cannot be removed by surgery
Dinaciclib (SCH727965, MK7965)	Pan-CDK	Phase I	Relapsed/refractory acute myeloid leukemia
		Phase I	Hematologic malignancies
		Phase I	Advanced solid tumors
		Phase I	Advanced breast cancer
CYC065	CDK2	Phase I	Relapsed/refractory AML or MDS
		Phase I/II	Advanced solid tumors and lymphoma
		Phase I	Relapsed/refractory CLL
		Phase I/II	Leukemia or myelodysplastic syndrome
Milciclib (PHA-848125)	CDK2	Phase II	Thymic carcinoma
		Phase II	Advanced non–small cell lung cancer
		Phase II	Unresectable/metastatic hepatocellular carcinoma
PF-07104091	CDK2	Phase I/II	Advanced or metastatic small-cell lung cancer Breast and ovarian cancers
		Phase I/II	Unresectable/metastatic hepatocellular carcinoma
PF-06873600	CDK2/4/6	Phase II	Hormone receptor-positive breast cancer HER2-negative breast cancer Triple-negative breast cancer Epithelial ovarian cancer Fallopian tube cancer Primary peritoneal cancer

Abbreviations: AML, acute myeloid leukemia; CLL, chronic lymphocytic leukemia; HER2, human epidermal growth factor receptor 2; IDH1/2, isocitrate dehydrogenase 1 or 2; MDS, myelodysplastic syndromes.
Note: The data are obtained from https://clinicaltrials.gov, which provides information on clinical trials conducted between 2018 and 2023.

various stages of drug development, including milciclib, AT7519M, CYC065, and others.

Summary and Prospect

In the past two decades, substantial progress has been achieved in the development of CDK inhibitors. Although CDK2 inhibitors have been in clinical development since the 1990s, most of them have primarily functioned as pan-CDK inhibitors. Consequently, early clinical trials were discontinued due to off-target effects and poor efficacy. Despite a long history of clinical studies, no CDK2 inhibitors have been approved for clinical use.[144] However, since 2015, the emergence of CDK4/6-selective inhibitors such as palbociclib,

abemaciclib, and ribociclib, has rekindled researchers' interest in CDK2 inhibitor research. This created a diverse range of novel scaffold compounds, significantly broadening the CDK2 inhibitor pool.

Classical CDK2 inhibitors bind to the conserved ATP catalytic pocket, mimicking the structure of the natural substrate ATP. This allows them to compete with ATP for the active site, hence they are categorized as ATP-competitive inhibitors. However, due to the highly conserved nature of amino acid residues in the ATP-binding pocket within the CDK family, these inhibitors lack selectivity toward specific kinases, potentially leading to off-target effects and resultant toxicity. In addition, the emergence of point mutations in amino acid residues of the binding site, or the activation of compensatory signaling pathways following the inhibition of kinase function, has hindered the development of the clinical applications of such inhibitors. Covalent inhibitors, also known as irreversible inhibitors, are characterized by the electrophilic warheads that form covalent bonds with specific nucleophilic amino acids at the ATP-binding site, thereby irreversibly inhibiting the kinase's activity. Although this enhances affinity and effectiveness to the target and prolongs therapeutic effect, significant challenges related to drug resistance and off-target effects persist. In addition, safety concerns arising from irreversible binding should be duly noted.[53,54,145] Allosteric inhibitors, classified as non-ATP competitive inhibitors, bind to allosteric pockets, which can be located near or far from the ATP-binding site. Unlike the ATP-binding site, the residual conservation of the allosteric site is significantly lower. Allosteric inhibitors exhibit selectivity toward various kinase subtypes by interacting with specific amino acid residues, effectively addressing drug resistance issues caused by Type I/II inhibitors. Moreover, they show promise *in vivo* pharmacology.[53,54,146] PROTAC technology facilitates the rapid degradation of pathogenic target proteins, requiring only a catalytic amount of drugs. It provides high selectivity, safety, and the capability to overcome drug resistance. Nonetheless, PROTAC molecules are characterized by a relatively high molecular weight, which may lead to reduced membrane permeability and limited oral bioavailability.[137,147]

Uncovering additional roles of CDK2 in cancer development, investigating cellular signaling cascades involving CDK2, facilitating biomarker discovery, and establishing a clear mechanism of action, is crucial to develop highly selective CDK2 inhibitors to reduce drug toxicity from off-target effects.[18,20] It is also important to search for and identify sensitive biomarkers and patients with suitable genetic backgrounds for the clinical application of CDK inhibitors. Concurrent targeting of CDK2 with other CDKs holds promise in expanding the range of drug development and reducing the emergence of drug resistance. Furthermore, CDK2 is involved in numerous oncogenic pathways, and combination therapy with CDK2 inhibitors shows more promise than single-drug treatment in clinical tumor therapy. Therefore, it is vital to develop rational and effective combination drug strategies to accelerate the progress of CDK2 inhibitors in clinical applications.

Funding
This work was supported by the National Natural Science Foundation of China (Grant Nos. 82003590, 22377068, and 92053105), Shandong Provincial Youth Innovation Team Development Program (Grant No. 2023KJ026), and the Taishan Scholars Program of Shandong Province (Grant No. tstp20230606).

Conflict of Interest
None declared.

References

1 Betzi S, Alam R, Martin M, et al. Discovery of a potential allosteric ligand binding site in CDK2. ACS Chem Biol 2011;6(05):492–501
2 Malumbres M. Cyclin-dependent kinases. Genome Biol 2014;15 (06):122
3 Hardcastle IR, Golding BT, Griffin RJ. Designing inhibitors of cyclin-dependent kinases. Annu Rev Pharmacol Toxicol 2002; 42:325–348
4 Galbraith MD, Bender H, Espinosa JM. Therapeutic targeting of transcriptional cyclin-dependent kinases. Transcription 2019; 10(02):118–136
5 Cao L, Chen F, Yang X, Xu W, Xie J, Yu L. Phylogenetic analysis of CDK and cyclin proteins in premetazoan lineages. BMC Evol Biol 2014;14:10
6 Ding L, Cao J, Lin W, et al. The roles of cyclin-dependent kinases in cell-cycle progression and therapeutic strategies in human breast cancer. Int J Mol Sci 2020;21(06):1960
7 Chou J, Quigley DA, Robinson TM, Feng FY, Ashworth A. Transcription-associated cyclin-dependent kinases as targets and biomarkers for cancer therapy. Cancer Discov 2020;10(03): 351–370
8 Jorda R, Hendrychová D, Voller J, Řezníčková E, Gucký T, Kryštof V. How selective are pharmacological inhibitors of cell-cycle-regulating cyclin-dependent kinases? J Med Chem 2018;61(20): 9105–9120
9 Vijayaraghavan S, Moulder S, Keyomarsi K, Layman RM. Inhibiting CDK in cancer therapy: current evidence and future directions. Target Oncol 2018;13(01):21–38
10 Yin X, Yu J, Zhou Y, et al. Identification of CDK2 as a novel target in treatment of prostate cancer. Future Oncol 2018;14(08): 709–718
11 First CDK 4/6 inhibitor heads to market. Cancer Discov 2015;5 (04):339–340
12 Ribociclib approved for advanced breast cancer. Cancer Discov 2017;7(05):OF3
13 Abemaciclib (Verzenio)–a third CDK 4/6 inhibitor for breast cancer. Med Lett Drugs Ther 2017;59(1533):185–186
14 Powell K, Prasad V. Concerning FDA approval of trilaciclib (Cosela) in extensive-stage small-cell lung cancer. Transl Oncol 2021;14(11):101206
15 Zhang H, Yan S, Zhan Y, et al. A mass balance study of [^{14}C] SHR6390 (dalpiciclib), a selective and potent CDK4/6 inhibitor in humans. Front Pharmacol 2023;14:1116073
16 Choo JR, Lee SC. CDK4-6 inhibitors in breast cancer: current status and future development. Expert Opin Drug Metab Toxicol 2018;14(11):1123–1138
17 Said MA, Abdelrahman MA, Abourehab MAS, Fares M, Eldehna WM. A patent review of anticancer CDK2 inhibitors (2017-present). Expert Opin Ther Pat 2022;32(08):885–898
18 Tadesse S, Anshabo AT, Portman N, et al. Targeting CDK2 in cancer: challenges and opportunities for therapy. Drug Discov Today 2020;25(02):406–413
19 Talapati SR, Nataraj V, Pothuganti M, et al. Structure of cyclin-dependent kinase 2 (CDK2) in complex with the specific and

potent inhibitor CVT-313. Acta Crystallogr F Struct Biol Commun 2020;76(Pt 8):350–356
20 Tadesse S, Caldon EC, Tilley W, Wang S. Cyclin-dependent kinase 2 inhibitors in cancer therapy: an update. J Med Chem 2019;62 (09):4233–4251
21 Tang J, Shewchuk LM, Sato H, Hasegawa M, Washio Y, Nishigaki N. Anilinopyrazole as selective CDK2 inhibitors: design, synthesis, biological evaluation, and X-ray crystallographic analysis. Bioorg Med Chem Lett 2003;13(18):2985–2988
22 De Bondt HL, Rosenblatt J, Jancarik J, Jones HD, Morgan DO, Kim SH. Crystal structure of cyclin-dependent kinase 2. Nature 1993; 363(6430):595–602
23 Gu Y, Rosenblatt J, Morgan DO. Cell cycle regulation of CDK2 activity by phosphorylation of Thr160 and Tyr15. EMBO J 1992; 11(11):3995–4005
24 Chohan TA, Qian H, Pan Y, Chen JZ. Cyclin-dependent kinase-2 as a target for cancer therapy: progress in the development of CDK2 inhibitors as anti-cancer agents. Curr Med Chem 2015;22(02): 237–263
25 Zheng N, Xu Y. Studies on protein function of cyclin-dependent kinase 2 and its inhibitors [in Chinese]. Chinese Journal of Cell Biology 2021;43(03):815–827
26 Ma T, Van Tine BA, Wei Y, et al. Cell cycle-regulated phosphorylation of p220(NPAT) by cyclin E/Cdk2 in Cajal bodies promotes histone gene transcription. Genes Dev 2000;14(18):2298–2313
27 Okuda M. The role of nucleophosmin in centrosome duplication. Oncogene 2002;21(40):6170–6174
28 Chen Z, Indjeian VB, McManus M, Wang L, Dynlacht BD. CP110, a cell cycle-dependent CDK substrate, regulates centrosome duplication in human cells. Dev Cell 2002;3(03):339–350
29 Saurus P, Kuusela S, Dumont V, et al. Cyclin-dependent kinase 2 protects podocytes from apoptosis. Sci Rep 2016;6:21664
30 Zhang DQ, Li JS, Zhang YM, Gao F, Dai RZ. Astragaloside IV inhibits angiotensin II-stimulated proliferation of rat vascular smooth muscle cells via the regulation of CDK2 activity. Life Sci 2018;200:105–109
31 Liu Q, Gao J, Zhao C, et al. To control or to be controlled? Dual roles of CDK2 in DNA damage and DNA damage response. DNA Repair (Amst) 2020;85:102702
32 Ying M, Shao X, Jing H, et al. Ubiquitin-dependent degradation of CDK2 drives the therapeutic differentiation of AML by targeting PRDX2. Blood 2018;131(24):2698–2711
33 Silva MC, Bodor DL, Stellfox ME, et al. Cdk activity couples epigenetic centromere inheritance to cell cycle progression. Dev Cell 2012;22(01):52–63
34 Hu S, Danilov AV, Godek K, et al. CDK2 inhibition causes anaphase catastrophe in lung cancer through the centrosomal protein CP110. Cancer Res 2015;75(10):2029–2038
35 Takada M, Zhang W, Suzuki A, et al. FBW7 loss promotes chromosomal instability and tumorigenesis via cyclin E1/ CDK2-mediated phosphorylation of CENP-A. Cancer Res 2017; 77(18):4881–4893
36 Chunder N, Wang L, Chen C, Hancock WW, Wells AD. Cyclin-dependent kinase 2 controls peripheral immune tolerance. J Immunol 2012;189(12):5659–5666
37 Lee S, Kim S, Chung H, Moon JH, Kang SJ, Park CG. Mesenchymal stem cell-derived exosomes suppress proliferation of T cells by inducing cell cycle arrest through p27kip1/Cdk2 signaling. Immunol Lett 2020;225:16–22
38 Hydbring P, Larsson LG. CDK2: a key regulator of the senescence control function of Myc. Aging (Albany NY) 2010;2(04):244–250
39 Gavet O, Pines J. Progressive activation of CyclinB1-CDK1 coordinates entry to mitosis. Dev Cell 2010;18(04):533–543
40 Zalzali H, Nasr B, Harajly M, et al. CDK2 transcriptional repression is an essential effector in p53-dependent cellular senescence-implications for therapeutic intervention. Mol Cancer Res 2015;13(01):29–40
41 Tang Z, Li L, Tang Y, et al. CDK2 positively regulates aerobic glycolysis by suppressing SIRT5 in gastric cancer. Cancer Sci 2018;109(08):2590–2598
42 Choi JS, Shin S, Jin YH, et al. Cyclin-dependent protein kinase 2 activity is required for mitochondrial translocation of Bax and disruption of mitochondrial transmembrane potential during etoposide-induced apoptosis. Apoptosis 2007;12(07):1229–1241
43 Jin YH, Yoo KJ, Lee YH, Lee SK. Caspase 3-mediated cleavage of p21WAF1/CIP1 associated with the cyclin A-cyclin-dependent kinase 2 complex is a prerequisite for apoptosis in SK-HEP-1 cells. J Biol Chem 2000;275(39):30256–30263
44 Huang H, Regan KM, Lou Z, Chen J, Tindall DJ. CDK2-dependent phosphorylation of FOXO1 as an apoptotic response to DNA damage. Science 2006;314(5797):294–297
45 Wang J, Yang T, Xu G, et al. Cyclin-dependent kinase 2 promotes tumor proliferation and induces radio resistance in glioblastoma. Transl Oncol 2016;9(06):548–556
46 Viegas DJ, Edwards TG, Bloom DC, Abreu PA. Virtual screening identified compounds that bind to cyclin dependent kinase 2 and prevent herpes simplex virus type 1 replication and reactivation in neurons. Antiviral Res 2019;172:104621
47 Guo S, Lei X, Chang Y, et al. SARS-CoV-2 hijacks cellular kinase CDK2 to promote viral RNA synthesis. Signal Transduct Target Ther 2022;7(01):400
48 Qin J, Huang T, Wang Z, et al. Bud31-mediated alternative splicing is required for spermatogonial stem cell self-renewal and differentiation. Cell Death Differ 2023;30(01):184–194
49 Faber EB, Wang N, John K, et al. Screening through lead optimization of high affinity, allosteric cyclin-dependent kinase 2 (CDK2) inhibitors as male contraceptives that reduce sperm counts in mice. J Med Chem 2023;66(03):1928–1940
50 Singh P, Patel RK, Palmer N, et al. CDK2 kinase activity is a regulator of male germ cell fate. Development 2019;146(21): dev180273
51 Lee SJ, Kim KH, Lee DJ, et al. MAST4 controls cell cycle in spermatogonial stem cells. Cell Prolif 2023;56(04):e13390
52 Hazlitt RA, Teitz T, Bonga JD, et al. Development of second-generation CDK2 inhibitors for the prevention of cisplatin-induced hearing loss. J Med Chem 2018;61(17):7700–7709
53 Zhao Z, Wu H, Wang L, et al. Exploration of type II binding mode: a privileged approach for kinase inhibitor focused drug discovery? ACS Chem Biol 2014;9(06):1230–1241
54 Attwood MM, Fabbro D, Sokolov AV, Knapp S, Schiöth HB. Trends in kinase drug discovery: targets, indications and inhibitor design. Nat Rev Drug Discov 2021;20(11):839–861
55 Pellerano M, Tcherniuk S, Perals Cet al. Targeting conformational activation of cdk2 kinase. Biotechnol J 2017;12(08)(e-pub ahead of print). DOI: 10.1002/biot.201600531
56 Anscombe E, Meschini E, Mora-Vidal R, et al. Identification and characterization of an irreversible inhibitor of CDK2. Chem Biol 2015;22(09):1159–1164
57 Coxon CR, Anscombe E, Harnor SJ, et al. Cyclin-dependent kinase (CDK) inhibitors: structure-activity relationships and insights into the CDK-2 selectivity of 6-substituted 2-arylaminopurines. J Med Chem 2017;60(05):1746–1767
58 Köprülüoğlu C, Dejmek M, Šála M, et al. Optimization of norbornyl-based carbocyclic nucleoside analogs as cyclin-dependent kinase 2 inhibitors. J Mol Recognit 2020;33(08):e2842
59 Park SJ, Kim E, Yoo M, et al. Synthesis and biological evaluation of N9-cis-cyclobutylpurine derivatives for use as cyclin-dependent kinase (CDK) inhibitors. Bioorg Med Chem Lett 2017;27(18):4399–4404
60 Yu Y, Ran D, Jiang J, et al. Discovery of novel 9*H*-purin derivatives as dual inhibitors of HDAC1 and CDK2. Bioorg Med Chem Lett 2019;29(16):2136–2140
61 Brooks EE, Gray NS, Joly A, et al. CVT-313, a specific and potent inhibitor of CDK2 that prevents neointimal proliferation. J Biol Chem 1997;272(46):29207–29211

62 Meijer L, Borgne A, Mulner O, et al. Biochemical and cellular effects of roscovitine, a potent and selective inhibitor of the cyclin-dependent kinases cdc2, cdk2 and cdk5. Eur J Biochem 1997;243(1–2):527–536

63 Cocco E, Lopez S, Black J, et al. Dual CCNE1/PIK3CA targeting is synergistic in CCNE1-amplified/PIK3CA-mutated uterine serous carcinomas *in vitro* and *in vivo*. Br J Cancer 2016;115(03): 303–311

64 Gray NS, Wodicka L, Thunnissen AM, et al. Exploiting chemical libraries, structure, and genomics in the search for kinase inhibitors. Science 1998;281(5376):533–538

65 Bettayeb K, Oumata N, Echalier A, et al. CR8, a potent and selective, roscovitine-derived inhibitor of cyclin-dependent kinases. Oncogene 2008;27(44):5797–5807

66 Rigas AC, Robson CN, Curtin NJ. Therapeutic potential of CDK inhibitor NU2058 in androgen-independent prostate cancer. Oncogene 2007;26(55):7611–7619

67 Ghia P, Scarfò L, Perez S, et al. Efficacy and safety of dinaciclib vs ofatumumab in patients with relapsed/refractory chronic lymphocytic leukemia. Blood 2017;129(13):1876–1878

68 Paruch K, Dwyer MP, Alvarez C, et al. Discovery of dinaciclib (SCH 727965): a potent and selective inhibitor of cyclin-dependent kinases. ACS Med Chem Lett 2010;1(05):204–208

69 Parry D, Guzi T, Shanahan F, et al. Dinaciclib (SCH 727965), a novel and potent cyclin-dependent kinase inhibitor. Mol Cancer Ther 2010;9(08):2344–2353

70 Feldmann G, Mishra A, Bisht S, et al. Cyclin-dependent kinase inhibitor Dinaciclib (SCH727965) inhibits pancreatic cancer growth and progression in murine xenograft models. Cancer Biol Ther 2011;12(07):598–609

71 Chen Z, Wang Z, Pang JC, et al. Multiple CDK inhibitor dinaciclib suppresses neuroblastoma growth via inhibiting CDK2 and CDK9 activity. Sci Rep 2016;6:29090

72 Lin SF, Lin JD, Hsueh C, Chou TC, Wong RJ. A cyclin-dependent kinase inhibitor, dinaciclib in preclinical treatment models of thyroid cancer. PLoS One 2017;12(02):e0172315

73 Moharram SA, Shah K, Khanum F, Marhäll A, Gazi M, Kazi JU. Efficacy of the CDK inhibitor dinaciclib *in vitro* and *in vivo* in T-cell acute lymphoblastic leukemia. Cancer Lett 2017;405:73–78

74 Hylsová M, Carbain B, Fanfrlík J, et al. Explicit treatment of active-site waters enhances quantum mechanical/implicit solvent scoring: inhibition of CDK2 by new pyrazolo[1,5-*a*]pyrimidines. Eur J Med Chem 2017;126:1118–1128

75 Hassan GS, Abdel Rahman DE, Nissan YM, Abdelmajeed EA, Abdelghany TM. Novel pyrazolopyrimidines: synthesis, *in vitro* cytotoxic activity and mechanistic investigation. Eur J Med Chem 2017;138:565–576

76 Cherukupalli S, Chandrasekaran B, Kryštof V, et al. Synthesis, anticancer evaluation, and molecular docking studies of some novel 4,6-disubstituted pyrazolo[3,4-*d*]pyrimidines as cyclin-dependent kinase 2 (CDK2) inhibitors. Bioorg Chem 2018;79:46–59

77 Cherukupalli S, Chandrasekaran B, Aleti RR, et al. Synthesis of 4, 6-disubstituted pyrazolo [3,4-*d*] pyrimidine analogues: cyclin-dependent kinase 2 (CDK2) inhibition, molecular docking and anticancer evaluation. J Mol Struct 2019;1176:538–551

78 Jorda R, Havlíček L, Šturc A, et al. 3,5,7-Substituted pyrazolo[4,3-d]pyrimidine inhibitors of cyclin-dependent kinases and their evaluation in lymphoma models. J Med Chem 2019;62(09): 4606–4623

79 Vymětalová L, Havlíček L, Šturc A, et al. 5-Substituted 3-isopropyl-7-[4-(2-pyridyl)benzyl]amino-1(2)*H*-pyrazolo[4,3-*d*]pyrimidines with anti-proliferative activity as potent and selective inhibitors of cyclin-dependent kinases. Eur J Med Chem 2016; 110:291–301

80 Vekariya MK, Vekariya RH, Brahmkshatriya PS, Shah NK. Pyrimidine-based pyrazoles as cyclin-dependent kinase 2 inhibitors: design, synthesis, and biological evaluation. Chem Biol Drug Des 2018;92(03):1683–1691

81 Cortese D, Chegaev K, Guglielmo S, et al. Synthesis and biological evaluation of n(2) -substituted 2,4-diamino-6-cyclohexylmethoxy-5-nitrosopyrimidines and related 5-Cyano-NNO-azoxy derivatives as cyclin-dependent kinase 2 (CDK2) inhibitors. ChemMedChem 2016;11(16):1705–1708

82 Wang Y, Chen Y, Cheng X, et al. Design, synthesis and biological evaluation of pyrimidine derivatives as novel CDK2 inhibitors that induce apoptosis and cell cycle arrest in breast cancer cells. Bioorg Med Chem 2018;26(12):3491–3501

83 Singh U, Chashoo G, Khan SU, et al. Design of novel 3-pyrimidinylazaindole CDK2/9 inhibitors with potent *in vitro* and *in vivo* antitumor efficacy in a triple-negative breast cancer model. J Med Chem 2017;60(23):9470–9489

84 Ajani H, Jansa J, Köprülüoğlu C, et al. Imidazo[1,2-*c*]pyrimidin-5 (6H)-one as a novel core of cyclin-dependent kinase 2 inhibitors: Synthesis, activity measurement, docking, and quantum mechanical scoring. J Mol Recognit 2018;31(09):e2720

85 Byth KF, Thomas A, Hughes G, et al. AZD5438, a potent oral inhibitor of cyclin-dependent kinases 1, 2, and 9, leads to pharmacodynamic changes and potent antitumor effects in human tumor xenografts. Mol Cancer Ther 2009;8(07):1856–1866

86 Diao PC, Lin WY, Jian XE, Li YH, You WW, Zhao PL. Discovery of novel pyrimidine-based benzothiazole derivatives as potent cyclin-dependent kinase 2 inhibitors with anticancer activity. Eur J Med Chem 2019;179:196–207

87 Freeman-Cook KD, Hoffman RL, Behenna DC, et al. Discovery of PF-06873600, a CDK2/4/6 inhibitor for the treatment of cancer. J Med Chem 2021;64(13):9056–9077

88 Alexander LT, Möbitz H, Drueckes P, et al. Type II inhibitors targeting CDK2. ACS Chem Biol 2015;10(09):2116–2125

89 Brasca MG, Amboldi N, Ballinari D, et al. Identification of *N*,1,4,4-tetramethyl-8-[4-(4-methylpiperazin-1-yl)phenyl]amino-4,5-dihydro-1*H*-pyrazolo[4,3-*h*]quinazoline-3-carboxamide (PHA-848125), a potent, orally available cyclin-dependent kinase inhibitor. J Med Chem 2009;52(16):5152–5163

90 William AD, Lee AC, Goh KC, et al. Discovery of kinase spectrum selective macrocycle (16*E*)-14-methyl-20-oxa-5,7,14,26-tetraazatetracyclo[19.3.1.1(2,6).1(8,12)]heptacosa-1(25),2(26),3,5,8 (27),9,11,16,21,23-decaene (SB1317/TG02), a potent inhibitor of cyclin dependent kinases (CDKs), Janus kinase 2 (JAK2), and fms-like tyrosine kinase-3 (FLT3) for the treatment of cancer. J Med Chem 2012;55(01):169–196

91 Siemeister G, Lücking U, Wengner AM, et al. BAY 1000394, a novel cyclin-dependent kinase inhibitor, with potent antitumor activity in mono- and in combination treatment upon oral application. Mol Cancer Ther 2012;11(10):2265–2273

92 Pennati M, Campbell AJ, Curto M, et al. Potentiation of paclitaxel-induced apoptosis by the novel cyclin-dependent kinase inhibitor NU6140: a possible role for survivin down-regulation. Mol Cancer Ther 2005;4(09):1328–1337

93 Chu XJ, DePinto W, Bartkovitz D, et al. Discovery of [4-Amino-2-(1-methanesulfonylpiperidin-4-ylamino)pyrimidin-5-yl](2,3-difluoro-6- methoxyphenyl)methanone (R547), a potent and selective cyclin-dependent kinase inhibitor with significant *in vivo* antitumor activity. J Med Chem 2006;49(22):6549–6560

94 Wang Y, Zhi Y, Jin Q, et al. Discovery of 4-((7*H*-pyrrolo[2,3-*d*] pyrimidin-4-yl)amino)-*N*-(4-((4-methylpiperazin-1-yl)methyl) phenyl)-1*H*-pyrazole-3-carboxamide (FN-1501), an FLT3- and CDK-kinase inhibitor with potentially high efficiency against acute myelocytic leukemia. J Med Chem 2018;61(04):1499–1518

95 Zhi Y, Wang Z, Yao C, et al. Design and synthesis of 4-(heterocyclic substituted amino)-1*H*-pyrazole-3-carboxamide derivatives and their potent activity against acute myeloid leukemia (AML). Int J Mol Sci 2019;20(22):5739

96 Cheng C, Yun F, Ullah S, Yuan Q. Discovery of novel cyclin-dependent kinase (CDK) and histone deacetylase (HDAC) dual inhibitors with potent *in vitro* and *in vivo* anticancer activity. Eur J Med Chem 2020;189:112073

97 Oudah KH, Najm MAA, Samir N, Serya RAT, Abouzid KAM. Design, synthesis and molecular docking of novel pyrazolo [1,5-*a*][1,3,5]triazine derivatives as CDK2 inhibitors. Bioorg Chem 2019;92:103239

98 Opoku-Temeng C, Dayal N, Hernandez DE, Naganna N, Sintim HO. Tetrahydro-3*H*-pyrazolo[4,3-*a*]phenanthridine-based CDK inhibitor. Chem Commun (Camb) 2018;54(36):4521–4524

99 Pfizer. A study to learn about the study medicine (called PF-07220060 in combination with pf-07104091) in participants with breast cancer and solid tumors. ClinicalTrials.gov identifier: NCT05 262400. Updated July 24, 2024. Accessed December 5, 2023 at: https://www.clinicaltrials.gov/study/NCT05262400#eligibility

100 Patel MR, Dejan Juric D, Henick BS, et al. VELA: A first-in-human phase 1/2 study of BLU-222, a potent, selective cyclin-dependent kinase (CDK) 2 inhibitor in patients with cyclin E1 gene (CCNE1)-amplified or CDK4/6 inhibitor-resistant advanced solid tumors [abstract]. Paper presented at: Proceedings of the 2022 San Antonio Breast Cancer Symposium; December 6–10, 2022; San Antonio, TX. Philadelphia, PA: AACR; Cancer Res 2023;83(5 suppl):Abstract nr OT3–23–01

101 Alec GT, John EB, Catherine D, et al. INX-315, a potent and selective CDK2 inhibitor, demonstrates robust antitumor activity in CCNE1-amplified cancers [abstract]. Paper presented at: Proceedings of the American Association for Cancer Research Annual Meeting 2023; Part 1 (Regular and Invited Abstracts); April 14–19, 2023; Orlando, FL. Philadelphia, PA: AACR; Cancer Res 2023;83(7_suppl):Abstract nr 5994

102 Chand S, Hansbury M, Lo Y, et al. Development of a CDK2-selective small molecule inhibitor INCB123667 for the treatment of CCNE1hi breast cancers [abstract]. Paper presented at: Proceedings of the American Association for Cancer Research Annual Meeting 2023; Part 1 (Regular and Invited Abstracts); April 14–19, 2023; Orlando, FL. Philadelphia, PA: AACR; Cancer Res 2023;83(7_suppl):Abstract nr 1143

103 Pfizer. PF-07104091 as a single agent and in combination therapy. ClinicalTrials.gov identifier: NCT04553133. Updated May 16, 2024. Accessed December 5, 2023 at: https://clinicaltrials.gov/study/NCT04553133

104 Patel H, Periyasamy M, Sava GP, et al. ICEC0942, an orally bioavailable selective inhibitor of cdk7 for cancer treatment. Mol Cancer Ther 2018;17(06):1156–1166

105 Santo L, Vallet S, Hideshima T, et al. AT7519, A novel small molecule multi-cyclin-dependent kinase inhibitor, induces apoptosis in multiple myeloma via GSK-3beta activation and RNA polymerase II inhibition. Oncogene 2010;29(16):2325–2336

106 Ferguson FM, Doctor ZM, Ficarro SB, et al. Discovery of covalent CDK14 inhibitors with Pan-TAIRE family specificity. Cell Chem Biol 2019;26(06):804–817.e12

107 McMillin DW, Delmore J, Negri J, et al. Molecular and cellular effects of multi-targeted cyclin-dependent kinase inhibition in myeloma: biological and clinical implications. Br J Haematol 2011;152(04):420–432

108 Misra RN, Xiao Hy, Rawlins DB, et al. 1*H*-Pyrazolo[3,4-*b*]pyridine inhibitors of cyclin-dependent kinases: highly potent 2,6-difluorophenacyl analogues. Bioorg Med Chem Lett 2003;13 (14):2405–2408

109 Brasca MG, Albanese C, Alzani R, et al. Optimization of 6,6-dimethyl pyrrolo[3,4-*c*]pyrazoles: identification of PHA-793887, a potent CDK inhibitor suitable for intravenous dosing. Bioorg Med Chem 2010;18(05):1844–1853

110 Xu X, Yao Q. Scaffold hopping approach to a new series of pyridine derivatives as potent inhibitors of CDK2. Arch Pharm (Weinheim) 2016;349(03):224–231

111 Wu YZ, Ying HZ, Xu L, et al. Design, synthesis, and molecular docking study of 3*H*-imidazole[4,5-*c*]pyridine derivatives as CDK2 inhibitors. Arch Pharm (Weinheim) 2018;351(06):e1700381

112 Bharate SB, Kumar V, Jain SK, et al. Discovery and preclinical development of IIIM-290, an orally active potent cyclin-dependent kinase inhibitor. J Med Chem 2018;61(04): 1664–1687

113 Hu X, Zhao H, Wang Y, Liu Z, Feng B, Tang C. Synthesis and biological evaluation of novel 5,6-dihydropyrimido[4,5-*f*]quinazoline derivatives as potent CDK2 inhibitors. Bioorg Med Chem Lett 2018;28(20):3385–3390

114 Arba M, Ihsan S, Ramadhan OA, Tjahjono DH. *In silico* study of porphyrin-anthraquinone hybrids as CDK2 inhibitor. Comput Biol Chem 2017;67:9–14

115 Abd El-Karim SS, Syam YM, El Kerdawy AM, Abdelghany TM. New thiazol-hydrazono-coumarin hybrids targeting human cervical cancer cells: synthesis, CDK2 inhibition, QSAR and molecular docking studies. Bioorg Chem 2019;86:80–96

116 Baltus CB, Jorda R, Marot C, et al. Synthesis, biological evaluation and molecular modeling of a novel series of 7-azaindole based tri-heterocyclic compounds as potent CDK2/Cyclin E inhibitors. Eur J Med Chem 2016;108:701–719

117 Mahajan P, Chashoo G, Gupta M, Kumar A, Singh PP, Nargotra A. Fusion of structure and ligand-based methods for identification of novel CDK2 inhibitors. J Chem Inf Model 2017;57(08): 1957–1969

118 Al-Otaibi FA, Bakhotmah DA. Synthesis and biological evaluation of new fluorine compounds bearing 4-amino-1,2,4-triazino [4,3-*b*]-1, 2, 4-triazin-8-one and the related derivatives as CDK2 inhibitors of tumor cell. Polycycl Aromat Compd 2020;42(02):623–634

119 Fanta BS, Mekonnen L, Basnet SKC, et al. 2-Anilino-4-(1-methyl-1*H*-pyrazol-4-yl)pyrimidine-derived CDK2 inhibitors as anticancer agents: design, synthesis & evaluation. Bioorg Med Chem 2023;80:117158

120 Fanta BS, Lenjisa J, Teo T, et al. Discovery of *N*,4-Di(1*H*-pyrazol-4-yl)pyrimidin-2-amine-derived CDK2 inhibitors as potential anticancer agents: design, synthesis, and evaluation. Molecules 2023;28(07):2951

121 Jing L, Tang Y, Goto M, Lee KH, Xiao Z. SAR study on N^2,N^4-disubstituted pyrimidine-2,4-diamines as effective CDK2/CDK9 inhibitors and antiproliferative agents. RSC Adv 2018;8(22): 11871–11885

122 Panicker RC, Chattopadhaya S, Coyne AG, Srinivasan R. Allosteric small-molecule serine/threonine kinase inhibitors. Adv Exp Med Biol 2019;1163:253–278

123 Roskoski R Jr. Cyclin-dependent protein serine/threonine kinase inhibitors as anticancer drugs. Pharmacol Res 2019;139:471–488

124 Martin MP, Alam R, Betzi S, Ingles DJ, Zhu JY, Schönbrunn E. A novel approach to the discovery of small-molecule ligands of CDK2. ChemBioChem 2012;13(14):2128–2136

125 Christodoulou MS, Caporuscio F, Restelli V, et al. Probing an allosteric pocket of CDK2 with small molecules. ChemMedChem 2017;12(01):33–41

126 Rastelli G, Anighoro A, Chripkova M, Carrassa L, Broggini M. Structure-based discovery of the first allosteric inhibitors of cyclin-dependent kinase 2. Cell Cycle 2014;13(14):2296–2305

127 Chen H, Zhao Y, Li H, et al. Break CDK2/Cyclin E1 interface allosterically with small peptides. PLoS One 2014;9(10):e109154

128 Hu Y, Li S, Liu F, Geng L, Shu X, Zhang J. Discovery of novel nonpeptide allosteric inhibitors interrupting the interaction of CDK2/cyclin A3 by virtual screening and bioassays. Bioorg Med Chem Lett 2015;25(19):4069–4073

129 Carlino L, Christodoulou MS, Restelli V, et al. Structure-activity relationships of hexahydrocyclopenta[c]quinoline derivatives as allosteric inhibitors of CDK2 and EGFR. ChemMedChem 2018;13 (24):2627–2634

130 Craven GB, Affron DP, Allen CE, et al. High-throughput kinetic analysis for target-directed covalent ligand discovery. Angew Chem Int Ed Engl 2018;57(19):5257–5261

131 Karthiga A, Tripathi SK, Shanmugam R, Suryanarayanan V, Singh SK. Targeting the cyclin-binding groove site to inhibit the catalytic activity of CDK2/cyclin A complex using p27(KIP1)-derived peptidomimetic inhibitors. J Chem Biol 2014;8(01):11–24

132 Premnath PN, Craig SN, Liu S, McInnes C. Benzamide capped peptidomimetics as non-ATP competitive inhibitors of CDK2 using the REPLACE strategy. Bioorg Med Chem Lett 2016;26 (15):3754–3760
133 Li HL, Ma Y, Ma Y, et al. The design of novel inhibitors for treating cancer by targeting CDC25B through disruption of CDC25B-CDK2/Cyclin A interaction using computational approaches. Oncotarget 2017;8(20):33225–33240
134 Song K, Liu X, Huang W, et al. Improved method for the identification and validation of allosteric sites. J Chem Inf Model 2017;57(09):2358–2363
135 Zhang J, Gan Y, Li H, et al. Inhibition of the CDK2 and cyclin A complex leads to autophagic degradation of CDK2 in cancer cells. Nat Commun 2022;13(01):2835
136 Yu B, Du Z, Zhang Y, Li Z, Bian J. Small-molecule degraders of cyclin-dependent kinase protein: a review. Future Med Chem 2022;14(03):167–185
137 Li K, Crews CM. PROTACs: past, present and future. Chem Soc Rev 2022;51(12):5214–5236
138 Zhou F, Chen L, Cao C, et al. Development of selective mono or dual PROTAC degrader probe of CDK isoforms. Eur J Med Chem 2020;187:111952
139 Teng M, Jiang J, He Z, et al. Development of CDK2 and CDK5 dual degrader TMX-2172. Angew Chem Int Ed Engl 2020;59(33): 13865–13870
140 Wang L, Shao X, Zhong T, et al. Discovery of a first-in-class CDK2 selective degrader for AML differentiation therapy. Nat Chem Biol 2021;17(05):567–575
141 Wei M, Zhao R, Cao Y, et al. First orally bioavailable prodrug of proteolysis targeting chimera (PROTAC) degrades cyclin-dependent kinases 2/4/6 *in vivo*. Eur J Med Chem 2021;209:112903
142 Hati S, Zallocchi M, Hazlitt R, et al. AZD5438-PROTAC: A selective CDK2 degrader that protects against cisplatin- and noise-induced hearing loss. Eur J Med Chem 2021;226:113849
143 Merck Sharp & Dohme LLC. A phase 3 study comparing dinaciclib versus ofatumumab in patients with refractory chronic lymphocytic leukemia (p07714). ClinicalTrials.gov identifier: NCT01580 228. Updated February 23, 2017. Accessed December 5, 2023 at: https://clinicaltrials.gov/study/NCT01580228
144 Rusina PV, Lisov AA, Denisova AA, Gandalipov ER, Novikov FN, Shtil AA. Clinical CDK2 inhibitors: trends to selectivity and efficacy. Recent Pat Anticancer Drug Discov 2022;18(02):102–107
145 Pecoraro C, Carbone D, Cascioferro SM, Parrino B, Diana P. Multi or single-kinase inhibitors to counteract drug resistance in cancer: what is new? Curr Med Chem 2023;30(07):776–782
146 Pan Y, Mader MM. Principles of kinase allosteric inhibition and pocket validation. J Med Chem 2022;65(07):5288–5299
147 Si R, Hai P, Zheng Y, et al. Discovery of intracellular self-assembly protein degraders driven by tumor-specific activatable bioorthogonal reaction. Eur J Med Chem 2023;257:115497